2012

Use of Pile Driving Analysis for Assessment of Axial Load Capacity of Piles

Rodrigo Salgado
Purdue University, rodrigo@ecn.purdue.edu

Yanbei Zhang
Purdue University, zhang508@purdue.edu

JOINT TRANSPORTATION RESEARCH PROGRAM

INDIANA DEPARTMENT OF TRANSPORTATION
AND PURDUE UNIVERSITY

USE OF PILE DRIVING ANALYSIS FOR ASSESSMENT OF AXIAL LOAD CAPACITY OF PILES

Rodrigo Salgado
Professor of Civil Engineering
School of Civil Engineering
Purdue University
Corresponding Author

Yanbei Zhang
Graduate Research Assistant
School of Civil Engineering
Purdue University

SPR-3378
Report Number: FHWA/IN/JTRP-2012/11
DOI: 10.5703/1288284314671

RECOMMENDED CITATION

Salgado, R., and Y. Zhang. *Use of Pile Driving Analysis for Assessment of Axial Load Capacity of Piles*. Publication FHWA/IN/JTRP-2012/11. Joint Transportation Research Program, Indiana Department of Transportation and Purdue University, West Lafayette, Indiana, 2012. doi: 10.5703/1288284314671.

CORRESPONDING AUTHOR

Professor Rodrigo Salgado
School of Civil Engineering
Purdue University
(765) 494-5030
rodrigo@purdue.edu

JOINT TRANSPORTATION RESEARCH PROGRAM

The Joint Transportation Research Program serves as a vehicle for INDOT collaboration with higher education institutions and industry in Indiana to facilitate innovation that results in continuous improvement in the planning, design, construction, operation, management and economic efficiency of the Indiana transportation infrastructure.
https://engineering.purdue.edu/JTRP/index_html

Published reports of the Joint Transportation Research Program are available at: http://docs.lib.purdue.edu/jtrp/

NOTICE

TECHNICAL REPORT STANDARD TITLE PAGE

1. Report No.	2. Government Accession No.	3. Recipient's Catalog No.
FHWA/IN/JTRP-2012/11		

4. Title and Subtitle	5. Report Date
Use of Pile Driving Analysis for Assessment of Axial Load Capacity of Piles	May 2012
	6. Performing Organization Code

7. Author(s)	8. Performing Organization Report No.
Rodrigo Salgado and Yanbei Zhang	FHWA/IN/JTRP-2012/11

9. Performing Organization Name and Address	10. Work Unit No.
Joint Transportation Research Program Purdue University 550 Stadium Mall Drive West Lafayette, IN 47907-2051	11. Contract or Grant No. SPR-3378

12. Sponsoring Agency Name and Address	13. Type of Report and Period Covered
Indiana Department of Transportation State Office Building 100 North Senate Avenue Indianapolis, IN 46204	Final Report
	14. Sponsoring Agency Code

15. Supplementary Notes
Prepared in cooperation with the Indiana Department of Transportation and Federal Highway Administration.

16. Abstract

Driven piles are commonly used in foundation engineering. Pile driving formulae, which directly relate the pile set per blow to the capacity of the pile, are commonly used to decide whether an installed pile will have the designed capacity. However, existing formulae have been proposed based on empirical observations and have not been validated scientifically, so some might over-predict pile capacity, while others may be too conservative. In this report, a more advanced and realistic model developed at Purdue University for dynamic pile driving analysis was used to develop more accurate pile driving formulae. These formulae are derived for piles installed in typical soil profiles: a floating pile in sand, an end-bearing pile in sand, a floating pile in clay, an end-bearing pile in clay and a pile crossing a normally consolidated clay layer and resting on a dense sand layer. The proposed driving formulae are validated through well documented case histories of driven piles. Comparison of the predictions from the proposed formulae with the results from static load tests, dynamic load tests and conventional formulae show that they produce reasonably accurate predictions of pile capacity based on pile set observations.

17. Key Words	18. Distribution Statement
pile design, numerical modeling, pile dynamics, dynamic analysis, pile driving formula, pile analysis, pile bearing capacity	No restriction. This document is available to the public through the National Technical Information Service Springfield, VA 22161

19. Security Classif. (of this report)	20. Security Classif. (of this page)	21. No. of Pages	22. Price
Unclassified	Unclassified	34	

Form DOT F 1700.7 (8-69)

EXECUTIVE SUMMARY

USE OF PILE DRIVING ANALYSIS FOR ASSESSMENT OF AXIAL LOAD CAPACITY OF PILES

Introduction

The dynamic response of a pile during driving is very complex, involving the interactions of the hammer, cushion, pile and soil during application of an impact load. The first analysis aimed at simulating a hammer blow on a pile was published in 1960. A revised, more realistic pile driving analysis was recently developed at Purdue University. Proper modeling of pile driving is important both for planning and inspecting pile driving operations. Reliable estimation of the load capacity of a driven pile based on the ease or difficulty with which the pile is driven allows an inspector to decide when pile driving can be discontinued.

One of the tools used to decide whether an installed pile will have the predicted capacity is the pile driving formula. Pile driving formulas directly relate the pile set per blow to the capacity of the pile, and, due to their simplicity, these formulas have been used often. However, existing formulas have been proposed based on empirical observations and have not been validated scientifically, so some formulas might over-predict pile capacity, while others may be too conservative. In this study we used the more advanced and realistic model developed at Purdue University for dynamic pile driving analysis to develop more accurate pile driving formulas, which consider both soil and pile variability. A review of the Purdue pile driving analysis method and a discussion on selection of model parameters to use in the analysis precedes the application of the analysis to typical soil profiles. Pile driving formulas are developed based on the results of these analyses for five ideal soil profiles: floating piles in sand and clay, end-bearing piles in sand and clay, and piles crossing clay resting on sand.

Well documented case histories of driven piles in Lagrange and Jasper Counties in Indiana are used to validate the proposed pile driving formulas. Comparison of the predictions of proposed formulas with the results of static load tests, dynamic load tests and conventional formulas show that the proposed model is capable of producing more reasonable and accurate predictions of pile capacity based on pile set observations.

Findings

We have developed pile driving formulas by fitting results of a realistic pile driving analysis performed for closed-ended steel pipe piles for five typical cases:

1. Floating piles in sand. The pile driving formula is expressed in this case in terms of five variables: the hammer efficiency, the normalized hammer weight, the normalized hammer drop height, the relative density of the sand and the pile set.
2. End-bearing piles in sand. The pile driving formula in this case is expressed in terms of five variables: the hammer efficiency, the normalized hammer weight, the normalized hammer drop height, the ratio of shaft to base relative density and the pile set.
3. Floating piles in normally consolidated clay. The pile driving formula in this case is expressed in terms of four variables: the hammer efficiency, the normalized hammer weight, the normalized hammer drop height and the normalized pile set.
4. Piles crossing a normally consolidated clay layer and resting on an over-consolidated clay layer. The pile driving formula in this case is expressed in terms of four variables: the hammer efficiency, the normalized hammer weight, the normalized hammer drop height and the normalized pile set.
5. Piles crossing a clay layer and resting on a dense sand layer. The proposed pile driving formula in this case is expressed in terms of five variables: the hammer efficiency, the normalized hammer weight, the normalized hammer drop height, the ratio of shaft relative density to base relative density and the pile set.

Implementation

Up to 80% of Indiana Department of Transportation (INDOT) projects lack the budget to allow dynamic load testing as a means to check the acceptability of driven piles, and therefore pile driving formulas are used. Similar numbers apply to other agencies and, indeed, private companies. Implementation of the results of this research will enable INDOT and other owners or contractors to take advantage of updated and improved pile driving formulas in smaller projects, leading to more economical piling.

Engineers can use the pile driving formulas proposed in this report in their work by following the following steps:

1. based on the soil profile information, decide which of the typical cases applies;
2. based on hammer information, estimate the hammer efficiency, the hammer weight and the hammer drop height;
3. estimate the soil properties to be used based on knowledge of the soil profile;
4. measure the pile set per blow at the end of pile driving;
5. take the value of the observed pile set into the corresponding pile driving formula to calculate the estimated capacity of the pile.

CONTENTS

LIST OF TABLES

LIST OF FIGURES

1. INTRODUCTION

1.1 Problem Statement

Driven piles are commonly used in foundation solutions. Because the pile driving process is variable and imposes significant changes to the state of the soil around the pile that are difficult to model, both the design and quality control of piling operations have been subject to considerable uncertainty and have been approached conservatively. It is desirable from a research point of view to develop reliable means to evaluate pile capacity during the design stage and then verify that that capacity is available during the installation process.

One of the methods to verify whether an installed pile will have the predicted capacity is through the use of pile driving formulas, which directly relate the pile set per blow with the capacity of the pile. Due to its simplicity, the Gates Formula (*1*) is commonly used by INDOT engineers in small- to medium-scale projects. There are other pile driving formulas available in the literature; a summary is given in Table 1.1. Most of these formulas are empirical in nature and may not be applicable to every soil deposit. These formulas have not been validated scientifically, so some might over-predict pile capacity, while others may be too conservative.

Research at Purdue University has recently produced advances in dynamic analysis of pile driving. The present study was motivated by a desire to put these analyses to use in pile driving verification. A number of projects exist with budgets that are too small to justify dynamic load tests. These projects would benefit from the use of pile driving formulas developed based on dynamic analysis. This report proposes a method by which such formulas can be developed and proposes formulas for a number of typical soil profiles. These formulas should be at the present time considered first results, requiring further validation.

1.2 Objectives and Organization

In Chapter 2, we briefly introduce the advanced soil reaction model and the solution scheme used for the advanced pile driving simulation model; we then discuss the selection of parameters for use in. In Chapter 3, we present the simulation results for typical soil profiles, and then develop pile driving formulas based on those results. In Chapter 4, we validate the formula by comparison with field test results (from static load tests and dynamic load tests on instrumented piles in well characterized soil) as well as with conventional pile driving formulas. Chapter 5 contains a summary of the main findings of this report.

TABLE 1.1
Summary of Pile Driving Formulas

Name	Equation
Canadian National Building Code	$Q_u = \frac{e_h E_h C_1}{s + C_2 C_3}$, $C_1 = C_4 = \frac{W_r + n^2(0.5 W_p)}{W_r + W_p}$, $C_2 = \frac{3Q_u}{2A}$, $C_3 = \frac{L}{E} + C_4$, $C_4 = 3.7 \times 10^{-10}\text{m}^2/\text{kN}$
Danish Formula (*3*)	$Q_u = \frac{e_h E_h}{s + C_1}$, $C_1 = \sqrt{\frac{e_{hE_h} L}{2AE}}$
Eytelwein Formula (*4*)	$Q_u = \frac{e_{hE_h}}{sC(W_p/W_r)}$, $C = 2.5\text{mm}$
Gates Formula (*1*)	$Q_u = a\sqrt{e_h E_h}(b - \log(s))$, $a = 104.5$, $b = 2.4$, s in mm
Janbu Formula (*3*)	$Q_u = \frac{e_h E_h}{k_u s}$, $k_u = C_d\left(1 + \sqrt{1 + \frac{\lambda}{C_d}}\right)$, $C_d = 0.75 + 0.15\frac{W_p}{W_r}$, $\lambda = \frac{e_h E_h L}{AEs^2}$
Modified ENR (*5*)	$Q_u = \left[\frac{1.25 e_h E_h}{s + C}\right]\left[\frac{W_r + n^2 W_p}{W_r + W_p}\right]$, $c = 2.5\text{mm}$
AASHTO (1990) (*6*)	$Q_u = \frac{2h(W_r + A_r p)}{s + C}$, $c = 2.5\text{mm}$
Navy-McKay Formula	$Q_u = \frac{e_h E_h}{s(1 + 0.3C_1)}$, $C_1 = \frac{W_p}{W_r}$
Pacific Coast Uniform Building Code	$Q_u = \frac{e_h E_h C_1}{s + C_2}$, $C_1 = \frac{W_r + k W_p}{W_r + W_p}$, $C_2 = \frac{Q_u L}{AE}$, $k = 0.25$ for steel piles, 0.10 for all other piles.

Source: (*2*).

2. PARAMETER SELECTION

2.1 Introduction

For many years, the state of practice in pile driving analysis has been the use of the analysis of Smith (*7*). Recently, Purdue engineers (*8*) proposed an analysis with a number of advancements over the Smith analysis. Initial evaluations of the Purdue analysis suggested it better predicted pile set given the static capacity and data for the pile and driving system. In this chapter, we will discuss how to choose values to use for each parameter in the Purdue dynamic driving analysis step by step.

The input parameters directly used in the shaft and base reaction models are:

1. Soil density ρ;
2. Small-strain shear modulus G_{max};
3. Poisson's ratio γ;
4. Pile dimensions, pile diameter B and pile length L;
5. Static unit shaft resistance, q_{sL};
6. Static unit base resistance, q_{bL};
7. Soil viscosity parameters, m_s, m_b, n_s and n_b.

These parameters can be related to fundamental soil variables, such as relative density D_R and critical state friction angle φ_c' for sandy soils and undrained shear strength s_u and over-consolidation ratio OCR for clayey soils.

2.2 Advanced Model for Pile Driving Analysis

The Purdue pile driving analysis is based on more advanced shaft and base reaction models, which are formulated based on the actual physics and mechanics of the pile driving problem, than are currently used in practice. Details of the analysis can be found in Loukidis et al. (*8*); the key elements of the analysis will be summarized in this section.

The shaft resistance of the pile is assumed to depend on the stiffness of a zone of highly localized strain (a shear band) that develops immediately next to the pile, on a zone of intermediate strains, where soil response is nonlinear, surrounding the shear band, and on a far field, in which strains are much smaller, further out. The shaft reaction model is shown in Figure 2.1.

To handle soil nonlinearity and hysteresis effectively, we will assume that the soil follows a hyperbolic stress-strain law in rate form:

$$\dot{\tau} = \frac{G_{\max}}{\left(1 + b_f \frac{|\tau - LI\tau_{rev}|}{(LI+1)\left|\mathrm{sgn}(\dot{\gamma})\cdot\tau_f - \tau\right|}\right)^2}\dot{\gamma} \qquad (2\text{-}1)$$

where:

τ_f = shear strength of the soil in simple shear conditions;

τ_{rev} = shear stress at the last stress reversal;

LI = loading index, equal to 0 for virgin loading and 1 for unloading and reloading;

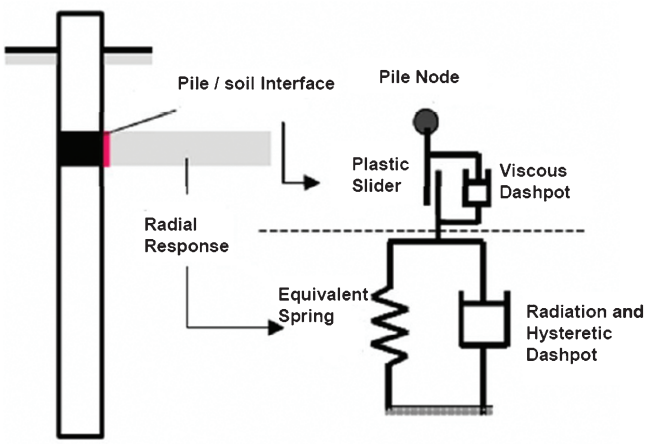

Figure 2.1 Soil model along pile shaft.

sgn = signum function, equal to 1 if $x>0$ and −1 if $x<0$;

G_{max} = small-strain shear modulus;

b_f = rate of degradation of the shear modulus.

A rheological model (*9*) represents the soil response within the shear band along the shaft wall. The proposed model consists of a plastic slider and a viscous dashpot connected in parallel and placed along the pile shaft wall. The strength of the plastic slider is equal to the static unit limit shaft resistance q_{sL}. Sliding initiates once the stress τ_s equals q_{sL}, at which point the viscous dashpot is activated. The reaction of the viscous dashpot is a power function of the relative velocity between the pile and soil near the pile shaft wall. The total resistance produced by this rheological model is given by:

$$\tau_{sf} = q_{sL}\left(1 + m_s\left(\dot{w}_{pile} - \dot{w}_1\right)^{n_s}\right) \qquad (2\text{-}2)$$

where m_s and n_s are input parameters that are discussed in detail in section 2.4.

The proposed base reaction model can take into account the nonlinear soil response below the pile base and the rate effect on base resistance and also distinguish between different types of damping.

The proposed base reaction model consists of a nonlinear spring connected in parallel to a radiation dashpot (Figure 2.2). By summing up the spring reaction $R_b^{(S)}$ and the radiation dashpot reaction $R_b^{(D)}$, the total base reaction is given as:

$$R_b = R_b^{(S)} + R_b^{(D)} = R_b^{(S)} + c_b\dot{w}_b \qquad (2\text{-}3)$$

where c_b is the radiation damping constant and $\dot{w}_b$ is the velocity of the pile base.

The nonlinear spring follows a hyperbolic type load-settlement law:

$$\dot{R}_b^{(S)} = \frac{K_{b,\max}}{\left(1 + b_{fb}\frac{|R_b - LI\cdot\tau_{b,rev}|}{(LI+1)\left|\mathrm{sgn}(\dot{w}_b)\cdot R_{bf} - R_b\right|}\right)^2}\dot{w}_b \qquad (2\text{-}4)$$

where:

$K_{b,max}$ = maximum base spring stiffness;

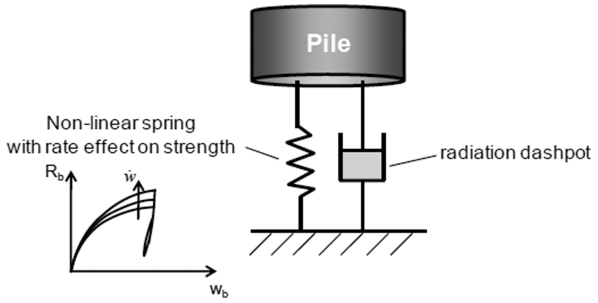

Figure 2.2 Proposed soil model at pile base.

R_{bf} = limit base capacity;

$R_{b,rev}$ = spring reaction R_b at last displacement reversal;

b_{fb} = rate of degradation of the base spring stiffness.

Inclusion of the rate effect in the model through R_{bf} yields a base resistance relationship similar to that for the limit shaft resistance:

$$R_{bf} = Q_{bL}(1 + m_b(\dot{w}_b)^{n_b}) \tag{2-5}$$

where m_b and n_b are input parameters controlling the soil viscosity.

The radiation dashpot coefficient for the pile base model is given as:

$$c_b = \frac{c_{Lysm} c_{emb} c_{hys}}{\left(1 + b_{fb} \dfrac{|R_b - LI \cdot \tau_{b,rev}|}{(LI+1)|\mathrm{sgn}(\dot{w}_b) \cdot R_{bf} - R_b|}\right)^2} \tag{2-6}$$

where:

c_{Lysm} = radiation dashpots coefficients of Lysmer's analog;

c_{emb} = depth factor for radiation damping;

c_{hys} = hysteretic damping effect on the radiation damping.

The solution scheme of 1D pile dynamic analysis is to discretize the pile into lumped masses with soil reactions applied to each lumped mass (Figure 2.3). The system of differential equations describing the problem is:

$$[M]\{\ddot{w}_{pile}\} + [C]\{\dot{w}_{pile}\} + [K]\{w_{pile}\} + \{R\} = 0 \tag{2-7}$$

where [M], [C] and [K] are the global mass matrix, global damping matrix and global stiffness matrix of the lumped mass system. The system of equations of motion (2-7) is solved using Newmark's algorithm.

2.3 Determination of Small-Strain Shear Modulus

The small-strain shear modulus for sandy soil can be estimated using the correlation proposed by Hardin and Black (*10*):

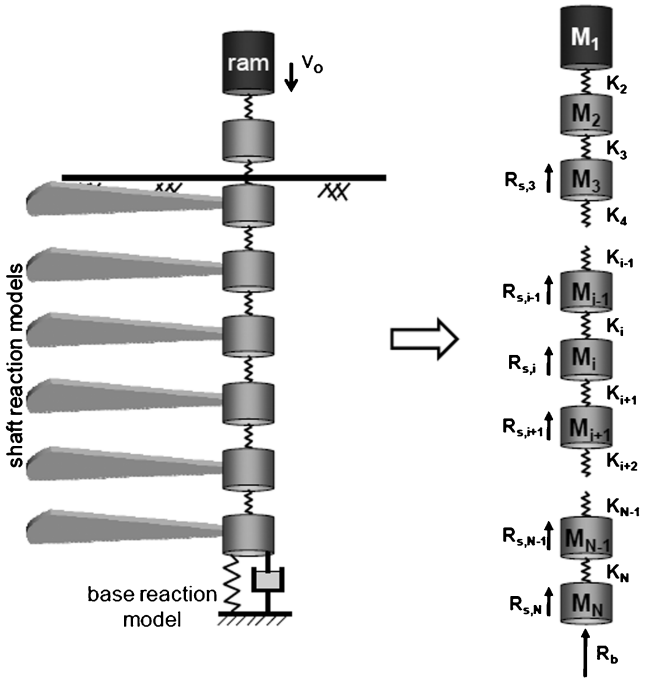

Figure 2.3 Lumped masses system of 1D dynamics analysis.

$$G_{\max} = 691 \frac{(2.17 - e)^2}{1 + e} \sqrt{p' p_a} \tag{2-8}$$

where e is the void ratio, p' is the mean effective stress, and p_a is a reference stress (the standard atmospheric pressure of 100kPa = 0.1MPa = 1kgf/cm^2 = 1tsf).

For clayey soils, the small-strain shear modulus takes the form (*11*):

$$G_{\max} = 323 \frac{(2.97 - e)^2}{1 + e} (OCR)^k \sqrt{p' p_a} \tag{2-9}$$

The power k to which the over-consolidation ratio OCR is raised is given in Table 2.1.

2.4 Determination of Soil Viscosity Parameters

The parameters n_s and n_b fall in a relatively narrow range, with most values being in the vicinity of 0.2 (*8*). Hence, a single value for $n_s = n_b = 0.2$ is selected independent of soil type.

For sands, we will assume $m_s = m_b = 0.3$ in accordance with Coyle and Gibson (*12*) and Randolph (*13*).

TABLE 2.1
Exponent k for Equation (2-9)

Plasticity Index (PI)	k
0	0.00
20	0.18
40	0.30
60	0.41
80	0.48
≥100	0.50

For clay, the parameters m_s and m_b are related to the undrained shear strength of the soil as proposed by Lee et al. (*14*):

$$m_s = 1.65 - 0.75\left(\frac{s_u}{p_a}\right) \geq 0 \tag{2-10}$$

$$m_b = 1.2 - 0.63\left(\frac{s_u}{p_a}\right) \geq 0 \tag{2-11}$$

2.5 Determination of Static Unit Shaft Resistance

For sand, the limit shaft resistance is evaluated using UWA-05 method (*15*). The UWA-05 design equations for shaft capacity of driven piles are expressed as follows:

$$q_{sL} = \frac{f_t}{f_c}\left\{0.03 q_c A_{r,eff}^{0.3}\left[\max\left(\frac{h}{B},2\right)^{-0.5}\right] + \Delta\sigma'_{rd}\right\}\tan\delta_f \tag{2-12}$$

$$A_{r,eff} = 1 - IFR\left(\frac{D_i}{D}\right)^2 \tag{2-13}$$

$$IFR_{mean} \approx \min\left[1, \left(\frac{D_i(m)}{1.5(m)}\right)^2\right] \tag{2-14}$$

$$\Delta\sigma'_{rd} = \frac{4G\Delta r}{D} \tag{2-15}$$

where:

δ_f = Constant volume interface friction angle;

h = Distance to the pile tip;

$\Delta\sigma'_{rd}$ = Change in radial stress due to loading stress path (dilation);

$\frac{f_t}{f_c}$ = 1 for compression and 0.75 for tension;

$G = 185 q_c q_{c1N}^{-0.75}$ with $q_{c1N}^{-0.75} = (q_c/p_a)/\left(\sigma'_{v0}/p_a\right)^{0.5}$;

p_a = A reference stress equal to 100kPa;

σ'_{v0} = In-situ vertical effective stress;

Δr = Dilation, assumed 0.02mm (*16*).

For clay, the limit shaft resistance is calculated through the α-method:

$$q_{sL} = \alpha s_u \tag{2-16}$$

The short term α_{ST} proposed by Basu et al. (*17*) is used:

$$\alpha_{ST} = 1.03\left[A_1 + (1 - A_1)\exp\left\{-\left(\frac{\sigma'_{v0}}{p_A}\right)\left(\phi_c - \phi_{r,\min}\right)^{A_2}\right\}\right] \tag{2-17}$$

where:

$$A_1 = \begin{cases} 0.75 \text{for} \left(\phi_c - \phi_{r,\min}\right) = 5^\circ \\ 0.43 \text{for} \left(\phi_c - \phi_{r,\min}\right) = 12^\circ \end{cases}$$

$$A_2 = 0.55 + 0.43\ln\left(\frac{s_u}{\sigma'_{v0}}\right)$$

$$A_3 = 0.64 + 0.40\ln\left(\frac{s_u}{\sigma'_{v0}}\right)$$

2.6 Determination of Static Unit Base Resistance

For sand, the static unit base resistance is related to cone penetration resistance, which is estimated using the equation proposed by Salgado and Prezzi (*18*):

$$q_{bL} = q_c = p_a 1.64\exp[0.1041\phi_c + (0.0264 - 0.0002\phi_c)D_R]\left(\frac{\sigma_h}{p_a}\right)^{0.841 - 0.0047 D_R} \tag{2-18}$$

For clay, the static unit base resistance is assumed to be ten times the undrained shear strength of the soil (*19*):

$$q_{bL} = 10 s_u \tag{2-19}$$

2.7 Determination of Other Parameters

The Poisson's ratio used in the model is the small-strain Poisson's ratio. Standard values of 0.15 and 0.22 can be used for sandy and clayey soils without much impact on the analysis results (*8*). The soil unit weight is computed from the relative density for sand. The unit weight used for normally consolidated clay is used as 17kN/m^3, and the unit weight for over-consolidated clay is 19kN/m^3.

3. PILE DRIVING FORMULAS

3.1 Introduction

In this chapter, we will simulate driving in five types of soil profile to develop the corresponding pile driving formulas. These general scenarios are those of a floating pile in sand, an end-bearing pile in sand, a floating pile in clay, an end-bearing pile in clay and a pile penetrating through a normally consolidated clay layer resting on a dense sand layer. For sand cases, we will control relative density and pile length to investigate their effects on the relation between the pile static capacity and pile set per blow. For clay cases, the over-consolidation ratio, the ratio of undrained shear strength over vertical effective stress for normally consolidated clay, and the pile length are used as variables. The pile static capacity ($Q_{10\%}$ for sand and Q_L for clay) is calculated as discussed in Chapter 2, and the pile set per blow is obtained from the numerical pile driving analysis.

Initially, analyses are done for the ICE-42S hammer, whose parameters are listed in Table 3.1. The pile is a steel close-ended pipe pile with an outer diameter of 356mm. The effects of the variability of hammer weight and drop height are taken into account in the final pile driving formula for each soil profile.

TABLE 3.1
Specifications of ICE-42S Hammer

Name	Value
Ram weight	4.09×10^3lbf (18.2kN)
Drop height	16.4ft (5m)
Maximum transferred energy	4.26×10^4lbf·ft (56.7kNm)
Energy ratio	62.4%

Source: (*20*).

3.2 Floating Pile in Sand

In this section, we consider the case of floating pile in a uniform sand layer, as shown in Figure 3.1. The relative density of the sand and the length of the pile are used as the two main variables to develop the pile driving formula. The relative density of the sand layer is allowed to vary from 10% to 90%, with 90% sand being an unrealistic case, except perhaps for very short piles, used to bound the results from above. In routine onshore practice, the driven pile length is usually in the range of 10m to 50m. To incorporate the length effect of the pile into the pile driving formula, simulations with pile length equal to 10m, 20m, 30m and 40m are done.

Table 3.2 summarizes the simulations performed to develop the pile driving formula for a floating pile in sand.

To properly consolidate the results of the simulations in to a useful equation, we will first normalize the pile set by dividing it by the pile length. The pile capacity and the normalized pile set can be fitted as a series of power functions in the form:

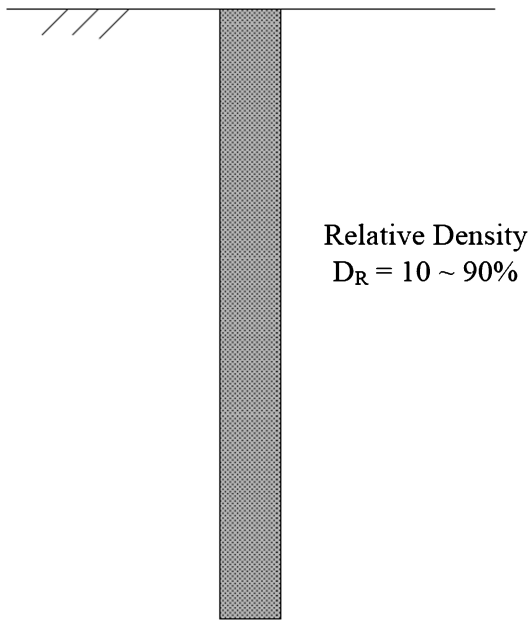

Figure 3.1 Floating pile in sand.

TABLE 3.2
Simulation Cases for Floating Pile in Sand

Name	Relative Density (%)	Pile Length (m)
Sand-FL 1	10	10, 20, 30, 40
Sand-FL 2	20	10, 20, 30, 40
Sand-FL 3	30	10, 20, 30, 40
Sand-FL 4	40	10, 20, 30, 40
Sand-FL 5	50	10, 20, 30, 40
Sand-FL 6	60	10, 20, 30, 40
Sand-FL 7	70	10, 20, 30, 40
Sand-FL 8	80	10, 20, 30, 40
Sand-FL 9	90	10, 20, 30, 40

$$Q_{10\%} = A\left(\frac{s}{L}\right)^B \tag{3-1}$$

The multiplier, exponent and coefficient of correlation for each case are listed in Table 3.3. To propose a unified pile driving formula in terms of relative density and normalized pile set, the parameter A for the power functions is fitted as an exponential function (Figure 3.2) of relative density, and the parameter B is fitted as a linear function (Figure 3.3) of relative density.

The final pile driving formula for floating piles in sand is given as:

$$Q_{10\%}\left(D_R, \frac{s}{L}\right) = \left(9.27\exp\left(3.11\frac{D_R}{100}\right)\right)\left(\frac{s}{L}\right)^{0.22\frac{D_R}{100}-0.68} \tag{3-2}$$

Figure 3.4 shows the plot of the proposed driving formula with all the simulated data points. To clearly evaluate the accuracy of the proposed formula, each case is plotted separately as shown in Figure 3.5 to Figure 3.13.

Equation (3-2) can be normalized with the reference p_a (100kPa = 0.1MPa = 1kgf/cm^2 = 1tsf) and the reference length L_R (1m = 3.28ft = 39.3in.) to obtain a nondimensional equation as follows:

TABLE 3.3
Values of *A* and *B* in Pile Driving Formula for Floating Pile in Sand

Name	*A*	*B*	R^2
Sand-FL 1	16.1	−0.63	0.998
Sand-FL 2	16.9	−0.64	0.999
Sand-FL 3	21.0	−0.63	1
Sand-FL 4	29.3	−0.60	1
Sand-FL 5	39.4	−0.58	1
Sand-FL 6	57.1	−0.55	1
Sand-FL 7	79.8	−0.53	1
Sand-FL 8	112	−0.50	1
Sand-FL 9	178	−0.46	0.999

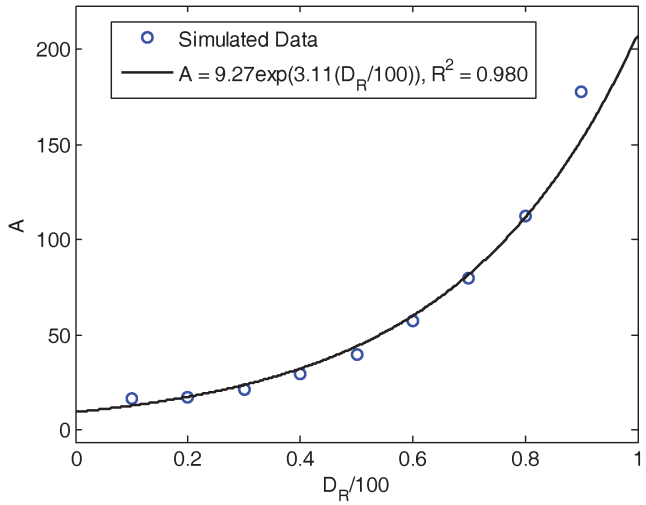

Figure 3.2 Multiplier *A* versus relative density for floating pile sand.

$$\frac{Q_{10\%}}{p_a L_R^2} = \left(0.093 \exp\left(3.11 \frac{D_R}{100}\right)\right)\left(\frac{s}{L}\right)^{0.22\frac{D_R}{100}-0.68} \quad (3\text{-}3)$$

3.3 End-Bearing Pile in Sand

The relative density of the sand layer along the pile shaft is assumed as 30% to simulate a relatively loose soil state. To characterize an end-bearing pile, the relative density of the pile base is from 40% to 90% (Figure 3.14). Table 3.4 summarizes the simulation cases performed to develop the pile driving formula for an end-bearing pile in sand.

Following the same technique discussed in section 3.2, the multiplier, exponent and coefficient of correlation of the power function for each case are listed in

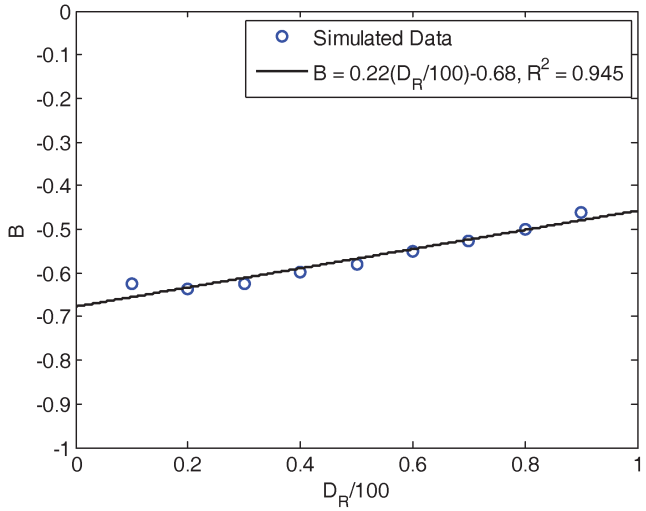

Figure 3.3 Exponent *B* versus relative density for a floating pile in sand.

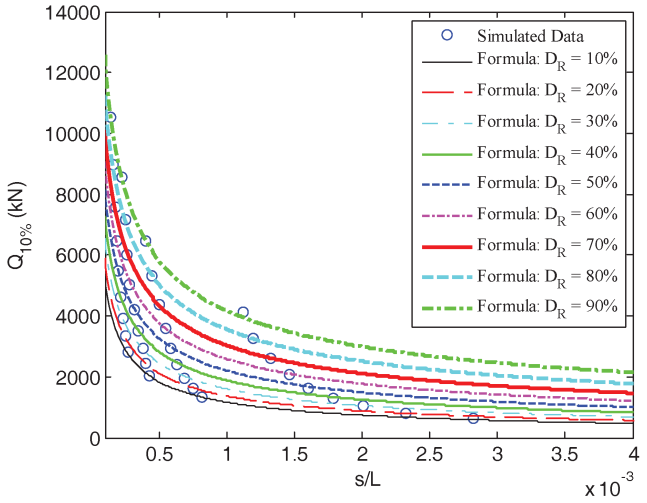

Figure 3.4 Simulated data (points) and proposed pile driving formulas (lines) for floating piles in sand.

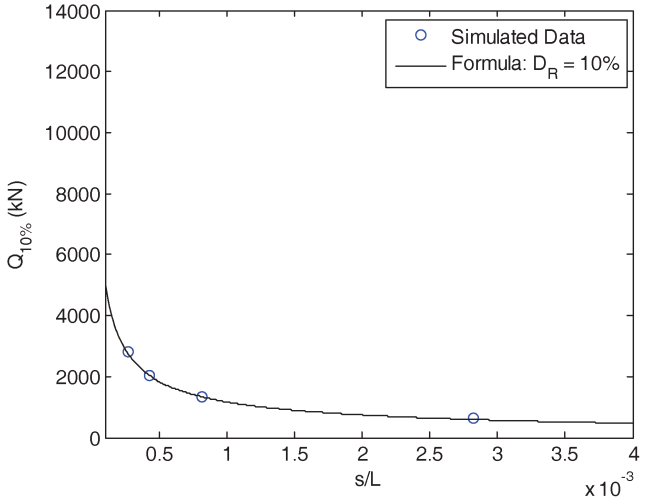

Figure 3.5 Pile driving formula with simulated data for D_R = 10%.

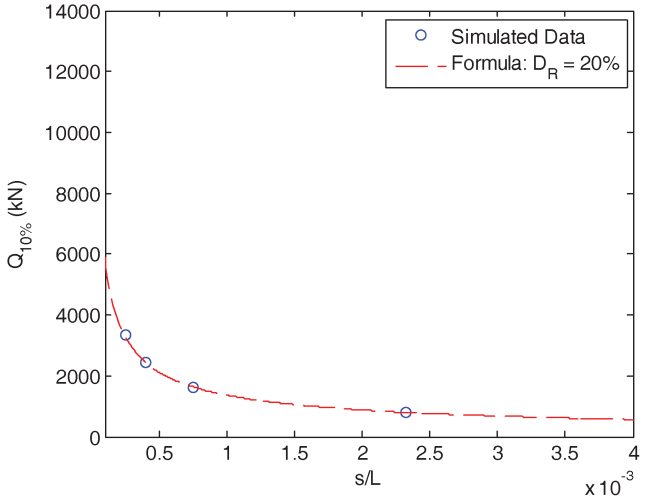

Figure 3.6 Pile driving formula with simulated data for D_R = 20%.

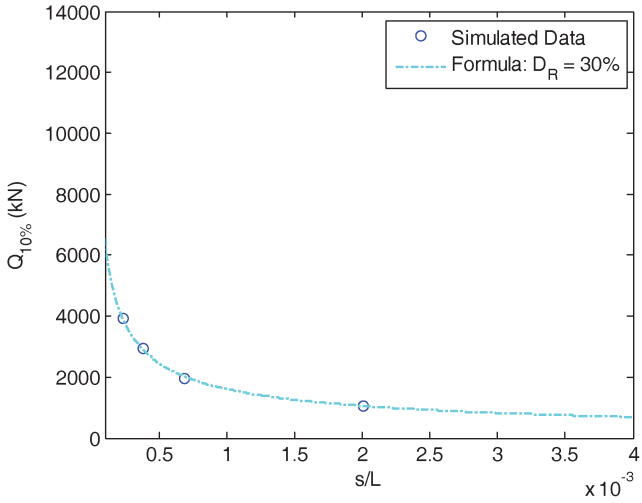

Figure 3.7 Pile driving formula with simulated data for D_R = 30%.

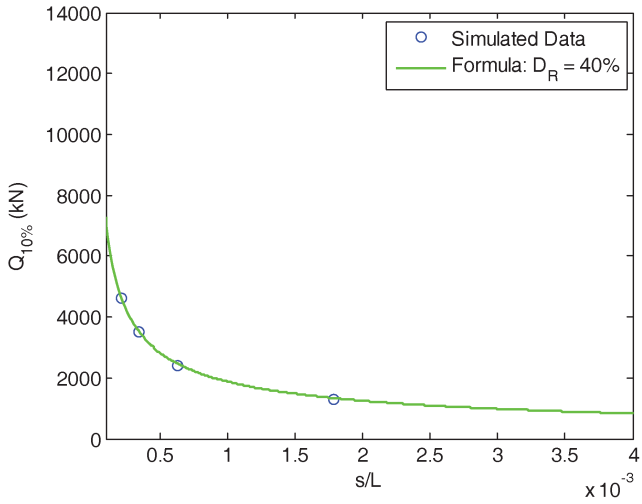

Figure 3.8 Pile driving formula with simulated data for D_R = 40%.

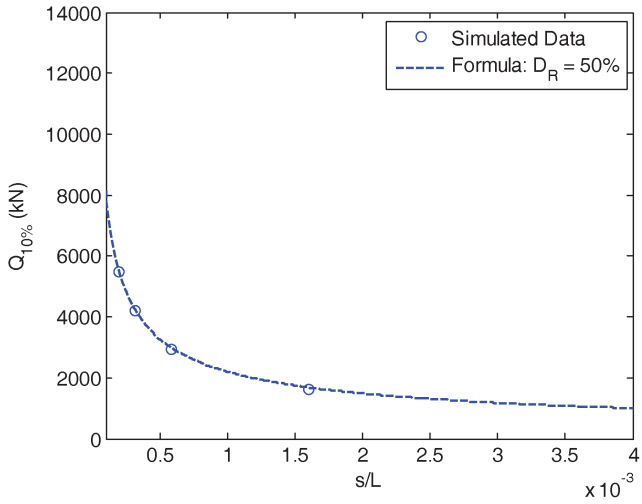

Figure 3.9 Pile driving formula with simulated data for D_R = 50%.

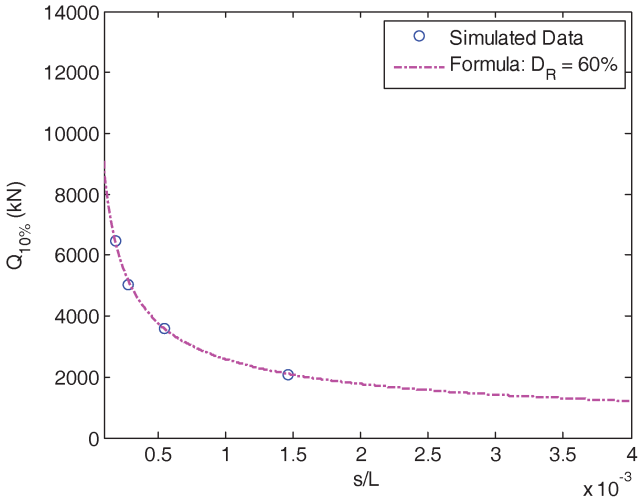

Figure 3.10 Pile driving formula with simulated data for D_R = 60%.

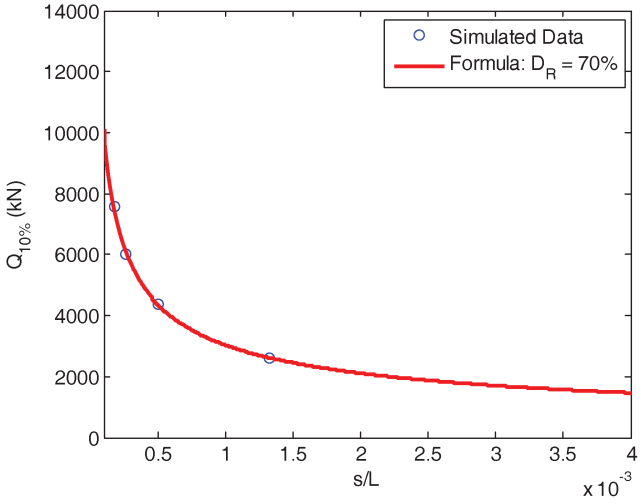

Figure 3.11 Pile driving formula with simulated data for D_R = 70%.

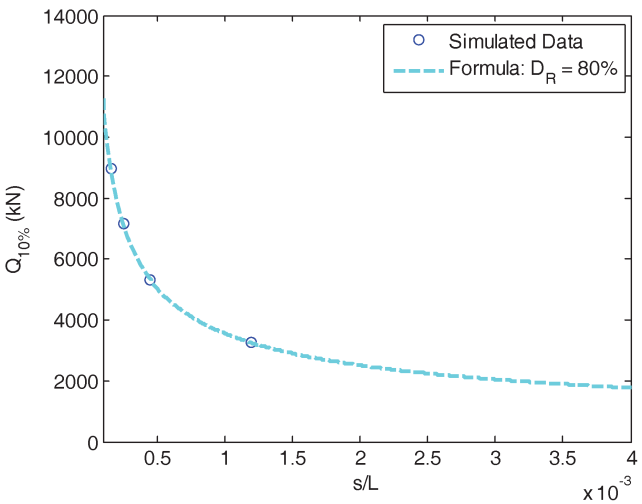

Figure 3.12 Pile driving formula with simulated data for D_R = 80%.

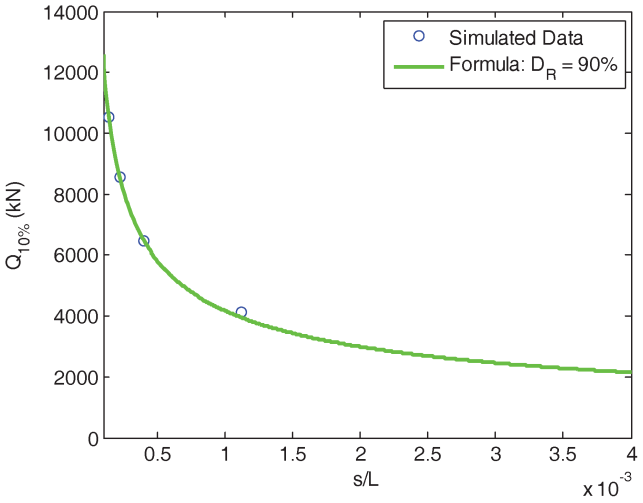

Figure 3.13 Pile driving formula with simulated data for D_R = 90%.

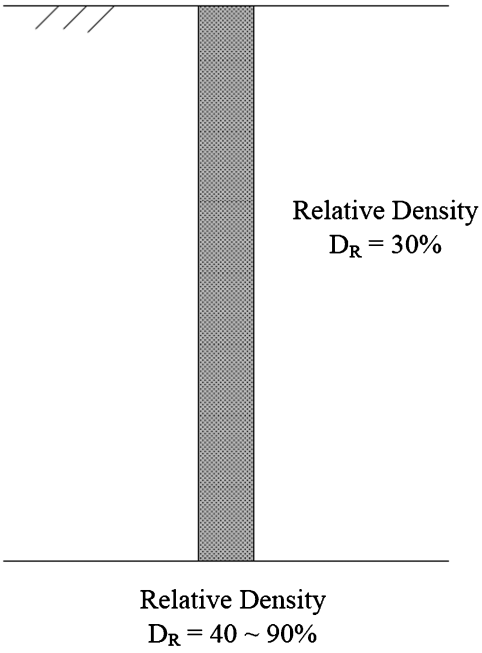

Figure 3.14 End-bearing pile in sand.

TABLE 3.4
Simulation Cases for End-Bearing Pile in Sand

Name	Base Relative Density (%)	Shaft Relative Density (%)	Pile Length (m)
Sand-EB 1	40	30	10, 20, 30, 40
Sand-EB 2	50	30	10, 20, 30, 40
Sand-EB 3	60	30	10, 20, 30, 40
Sand-EB 4	70	30	10, 20, 30, 40
Sand-EB 5	80	30	10, 20, 30, 40
Sand-EB 6	90	30	10, 20, 30, 40

TABLE 3.5
Parameters for Power Functions for End-Bearing Pile in Sand

Name	*A*	*B*	R^2
Sand-EB 1	24.3	−0.61	0.999
Sand-EB 2	32.7	−0.59	0.999
Sand-EB 3	48.7	−0.55	0.999
Sand-EB 4	69.7	−0.52	0.998
Sand-EB 5	99.6	−0.49	0.997
Sand-EB 6	153	−0.45	0.995

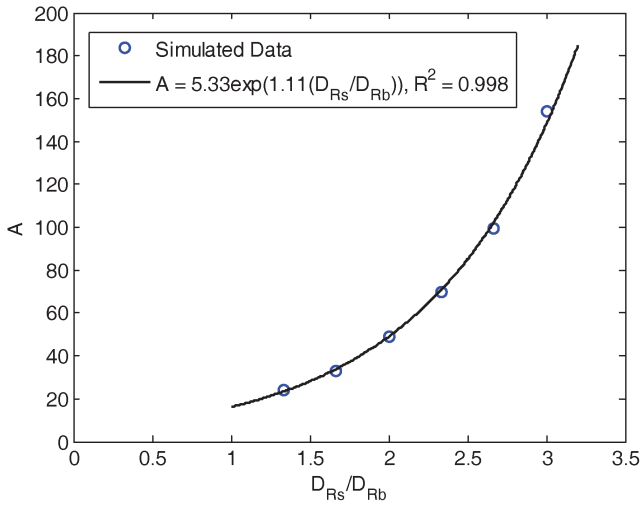

Figure 3.15 Multiplier *A* versus relative density ratio for end-bearing pile in sand.

Table 3.5. The regression of the multiplier and exponent for all the cases are shown in Figure 3.15 and Figure 3.16, which aim to relate them to the base-shaft relative density ratio.

The final pile driving formula for an end-bearing pile in sand is:

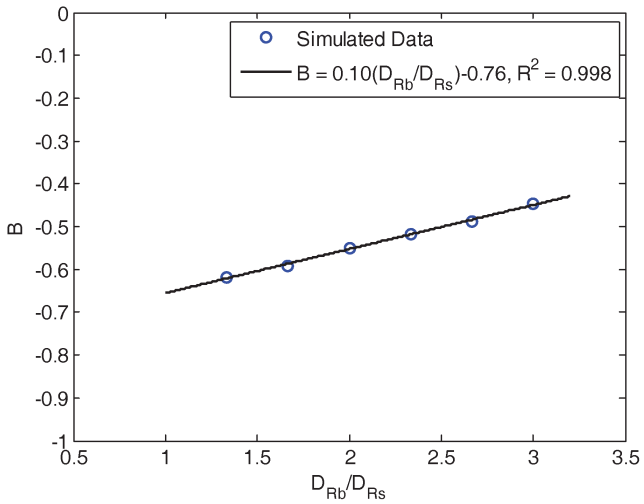

Figure 3.16 Exponent *B* versus relative density ratio for end-bearing pile in sand.

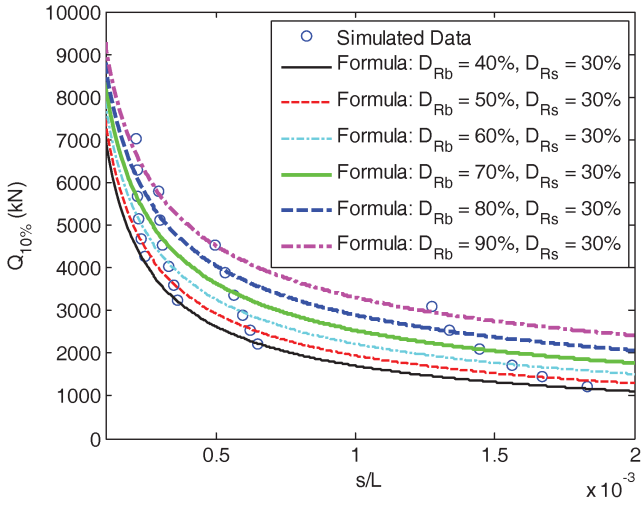

Figure 3.17 Simulated data (points) and proposed pile driving formulas (lines) for end-bearing piles in sand.

$$Q_{10\%}\left(\frac{D_{R_{base}}}{D_{R_{shaft}}},\frac{s}{L}\right)= \left(5.33\exp\left(1.11\frac{D_{R_{base}}}{D_{R_{shaft}}}\right)\right)\left(\frac{s}{L}\right)^{0.10\frac{D_{R_{base}}}{D_{R_{shaft}}}-0.76} \tag{3-4}$$

Equation (3-4) can be normalized with respect to the reference stress p_a and the reference length L_R to obtain a nondimensional equation as:

$$\frac{Q_{10\%}}{p_a L_R^2}=\left(0.053\exp\left(1.11\frac{D_{R_{base}}}{D_{R_{shaft}}}\right)\right)\left(\frac{s}{L}\right)^{0.10\frac{D_{R_{base}}}{D_{R_{shaft}}}-0.76} \tag{3-5}$$

Figure 3.17 shows the plot of the proposed driving formula together with all the simulated data. To clearly see the accuracy of the proposed formula, we plot the formula with simulated data for each case separately in Figure 3.18 through Figure 3.23.

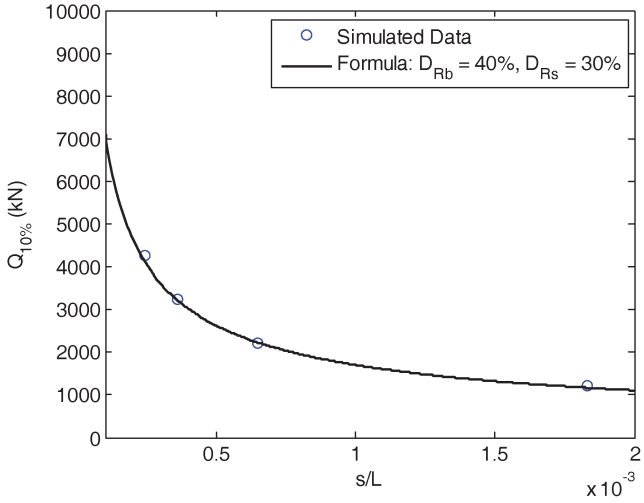

Figure 3.18 Proposed pile driving formula for end-bearing pile in sand: D_{Rb} = 40%.

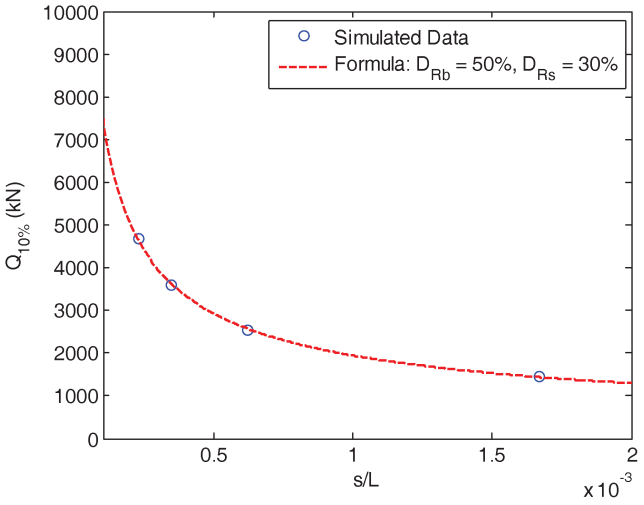

Figure 3.19 Proposed pile driving formula for end-bearing pile in sand: D_{Rb} = 50%.

3.4 Floating Pile in Clay

A constant ratio of the undrained shear strength over vertical effective stress s_u/σ_v' is assumed for a normally consolidated clay layer to simulate the floating pile in clay as shown in Figure 3.24. Table 3.6 summarizes the simulation cases considered to develop the pile driving formula. For each case, we use a different pile length in the 10m to 40m range.

The form for the pile driving formula for a floating pile in clay is:

$$Q_L\left(\frac{s_u}{\sigma_v'},\frac{s}{L}\right)=\left(34.10\frac{s_u}{\sigma_v'}+2.55\right)\left(\frac{s}{L}\right)^{0.67\frac{s_u}{\sigma_v'}-1.29} \tag{3-6}$$

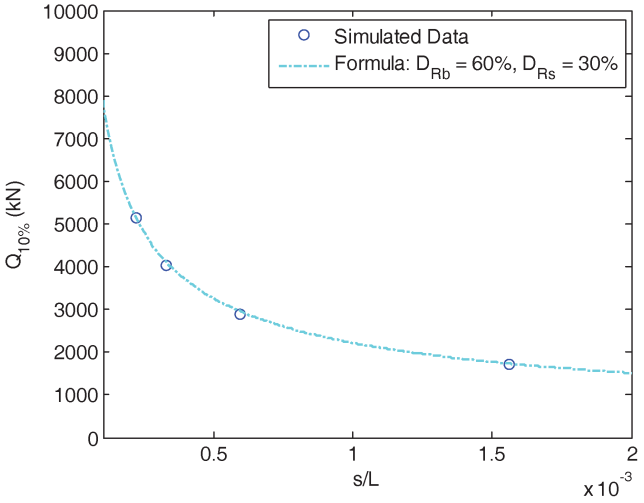

Figure 3.20 Proposed pile driving formula for end-bearing pile in sand: D_{Rb} = 60%.

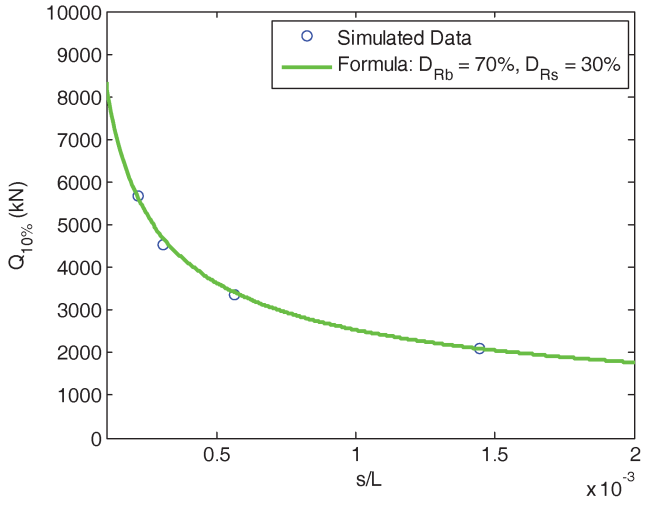

Figure 3.21 Proposed pile driving formula for end-bearing pile in sand: D_{Rb} = 70%.

Equation (3-6) can be normalized with the reference stress p_a and the reference length L_R as follows:

$$\frac{Q_L}{p_a L_R^2} = \left(0.34\frac{s_u}{\sigma_v'} + 0.026\right)\left(\frac{s}{L}\right)^{0.67\frac{s_u}{\sigma_v'} - 1.29} \tag{3-7}$$

Figure 3.25 shows the corresponding plot with simulated data. In Figure 3.25, the pile capacities for different s_u/σ_v' at the same pile set do not vary much. To maximize ease of use by engineers, a single equation is used to represent the entire range of conditions assumed:

$$Q_L(s) = 10.94 s^{-1.12} \tag{3-8}$$

The nondimensional form of Equation (3-8) is:

$$\frac{Q_L}{p_a L_R^2} = 0.11\left(\frac{s}{L_R}\right)^{-1.12} \tag{3-9}$$

where L_R is the reference length (1m=3.28ft).

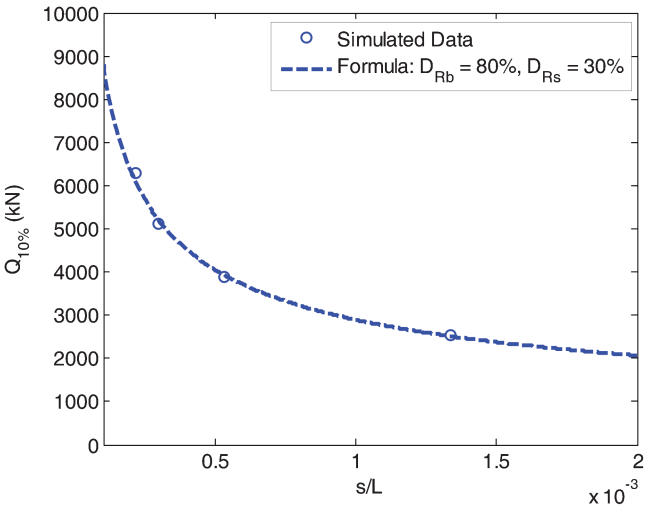

Figure 3.22 Proposed pile driving formula for end-bearing pile in sand: D_{Rb} = 80%.

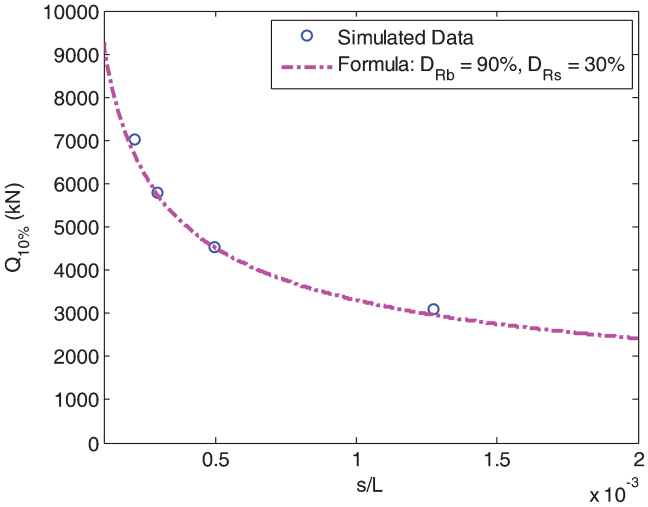

Figure 3.23 Proposed pile driving formula for end-bearing pile in sand: D_{Rb} = 90%.

TABLE 3.6
Simulation Cases for Floating Pile in Clay

Name	$\frac{s_u}{\sigma_v'}$	Pile Length (m)
Clay-FL 1	0.20	10, 20, 30, 40
Clay-FL 2	0.23	10, 20, 30, 40
Clay-FL 3	0.25	10, 20, 30, 40
Clay-FL 4	0.28	10, 20, 30, 40
Clay-FL 5	0.30	10, 20, 30, 40

The coefficient of correlation of (3-8) with all the simulated data is close to 0.987 as shown in Figure 3.26, which means that the simple form of (3-8) is accurate enough to substitute for the more complex form (3-6).

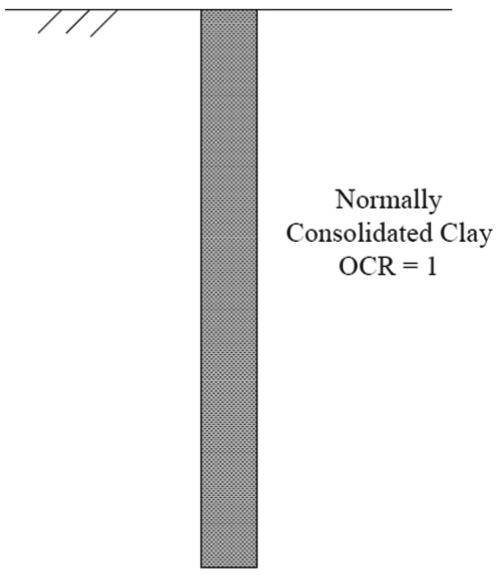

Figure 3.24 Floating pile in clay.

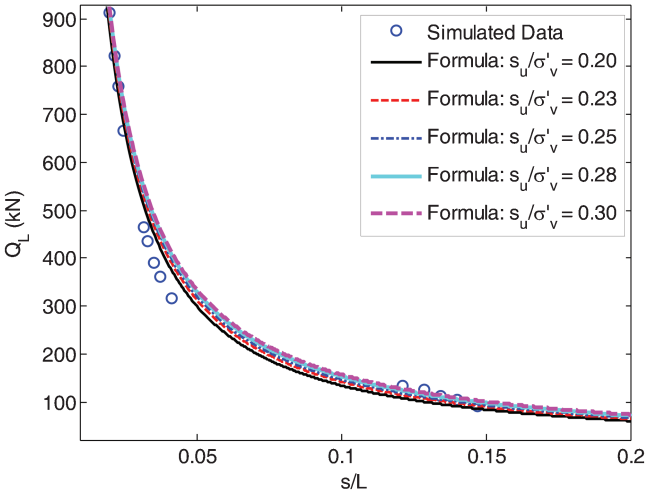

Figure 3.25 Simulated data (points) and proposed pile driving formulas (lines) for floating piles in clay.

3.5 End-Bearing Pile in Clay

To simulate the case of an end-bearing pile in clay, the pile is simulated to penetrate through a normally consolidated clay layer and rest on an over-consolidated clay layer with higher *OCR* as shown in Figure 3.27. Table 3.7 summarizes all the cases considered.

If we were to fit the data separately for each value of *OCR*, for *OCR* = 4, the pile driving formula is in the form:

$$Q_L\left(\frac{s_u}{\sigma_v'},\frac{s}{L}\right)=\left(15.78\frac{s_u}{\sigma_v'}+1.32\right)\left(\frac{s}{L}\right)^{0.13\frac{s_u}{\sigma_v'}-0.73} \tag{3-10}$$

Equation (3-10) can be normalized with respect to the reference stress p_a and the reference length L_R as follows:

$$\frac{Q_L}{p_a L_R^2}=\left(0.16\frac{s_u}{\sigma_v'}+0.013\right)\left(\frac{s}{L}\right)^{0.13\frac{s_u}{\sigma_v'}-0.73} \tag{3-11}$$

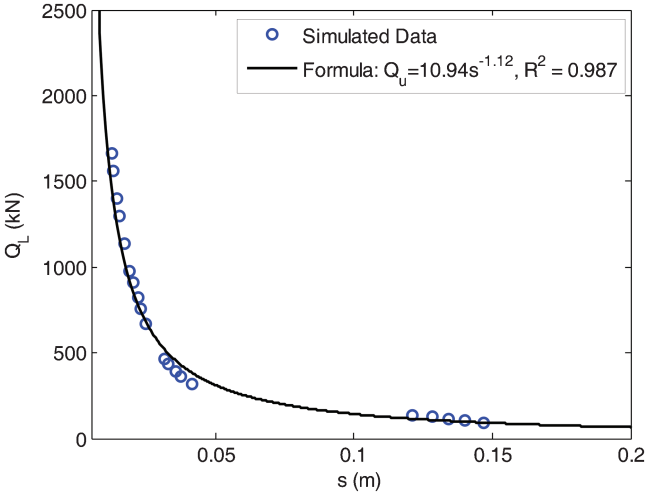

Figure 3.26 Pile driving formula for floating pile in clay.

TABLE 3.7
Simulation Cases for End-Bearing Pile in Clay

Name	*OCR*	$\frac{s_u}{\sigma_v'}$	Pile Length (m)
Clay-EB 1	4	0.20	10, 20, 30, 40
Clay-EB 2	4	0.23	10, 20, 30, 40
Clay-EB 3	4	0.25	10, 20, 30, 40
Clay-EB 4	4	0.28	10, 20, 30, 40
Clay-EB 5	4	0.30	10, 20, 30, 40
Clay-EB 6	10	0.20	10, 20, 30, 40
Clay-EB 7	10	0.23	10, 20, 30, 40
Clay-EB 8	10	0.25	10, 20, 30, 40
Clay-EB 9	10	0.28	10, 20, 30, 40
Clay-EB 10	10	0.30	10, 20, 30, 40

For *OCR* = 10, the pile driving formula has the form:

$$Q_L\left(\frac{s_u}{\sigma_v'},\frac{s}{L}\right)=\left(35.26\frac{s_u}{\sigma_v'}-2.27\right)\left(\frac{s}{L}\right)^{0.51\frac{s_u}{\sigma_v'}-0.80} \tag{3-12}$$

The nondimensional form of Equation (3-12) is:

$$\frac{Q_L}{p_a L_R^2}=\left(0.35\frac{s_u}{\sigma_v'}-0.028\right)\left(\frac{s}{L}\right)^{0.51\frac{s_u}{\sigma_v'}-0.80} \tag{3-13}$$

As shown in Figure 3.28, all the data points follow the trend of a single power function with coefficient of correlation equal to 0.975 regardless of the value of the over-consolidation ratio. Thus, we propose a simpler equation as the driving formula for end-bearing piles in clay:

$$Q_L=7.90s^{-1.18} \tag{3-14}$$

The nondimensional form of Equation (3-14) is proposed as:

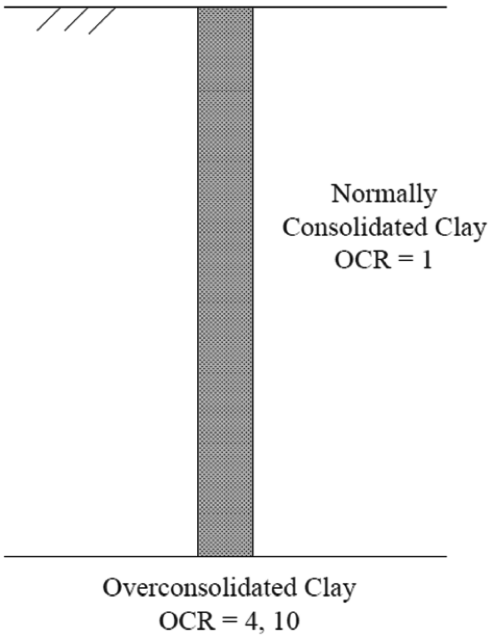

Figure 3.27 End-bearing pile in clay.

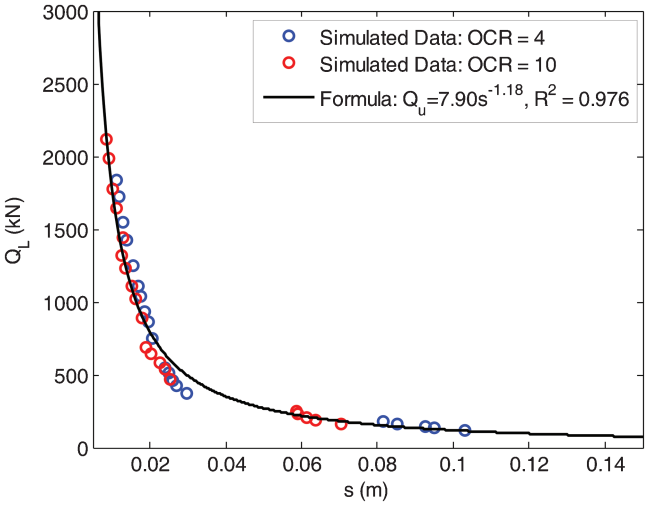

Figure 3.28 Simulated data (points) and proposed pile driving formula (line) of all OCR values for end-bearing pile in clay.

$$\frac{Q_L}{p_a L_R^2} = 0.079\left(\frac{s}{L_R}\right)^{-1.18} \tag{3-15}$$

3.6 Clay over Sand

In this case, the pile is assumed to cross a normally consolidated clay layer and rest on a relatively dense sand layer. The relative density of the base sand layer varies from 40% to 90%. To incorporate the effect of the pile length into the pile driving formula, the pile length used is 10m, 20m, 30m and 40m (Figure 3.29).

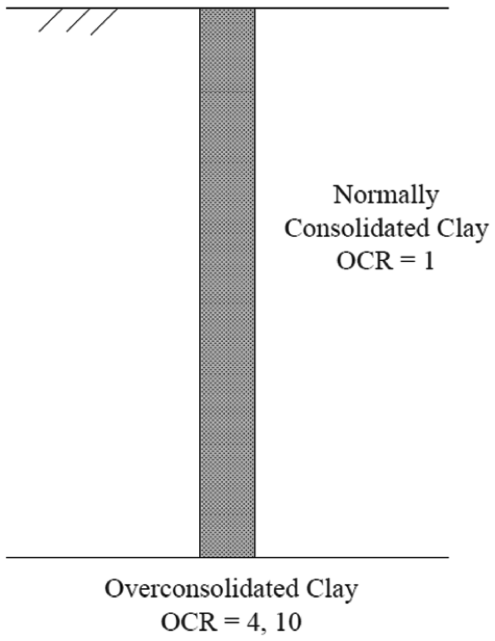

Figure 3.29 End-bearing pile penetrated through clay and rested on sand.

Table 3.8 summarizes the simulation cases performed to develop the pile driving formula for this case. The multiplier, exponent and coefficient of correlation of the power function for each case are listed in Table 3.9. The regression of the multiplier and exponent for all the cases are shown in Figure 3.30 and Figure 3.31. The coefficient of correlation of multiplier A and exponent B among all cases are both as high as 0.988.

The final pile driving formula for a pile crossing a clay layer and bearing on a sand layer can be written as:

$$Q_{10\%}\left(D_R, \frac{s}{L}\right) = \left(2.81\exp\left(4.22\frac{D_R}{100}\right)\right)\left(\frac{s}{L}\right)^{0.40\frac{D_R}{100}-0.77} \tag{3-16}$$

Equation (3-16) can be normalized with respect to the reference stress p_a and the reference length L_R to obtain this nondimensional form:

$$\frac{Q_{10\%}}{p_a L_R^2} = \left(0.028\exp\left(4.22\frac{D_R}{100}\right)\right)\left(\frac{s}{L}\right)^{0.40\frac{D_R}{100}-0.77} \tag{3-17}$$

Figure 3.32 shows the plot of the proposed driving formulas (lines) together with all the simulated data (points).

3.7 Effect of Hammer Weight and Drop Height

The pile driving formulas proposed in Section 3.2 to 3.6 are developed by using an ICE-42S hammer with the following properties: 18.2kN hammer weight, 5m drop height and 62.4% hammer efficiency. In practice, a variety of hammers, each with its own hammer weight and drop height could be used in a given pile driving project. A general pile driving formula needs to contain hammer parameters. In order to include hammer parameters in the pile driving formulas developed earlier, we have considered six combinations of hammer weights and drop heights (listed in Table 3.10). The reference force W_R (100kN = 2.25×10^3lbf = 22.5kips) and the reference length L_R (1m = 3.28ft = 39.3in.) are used to non-dimensionalize the pile driving formulas.

TABLE 3.8
Simulation Cases for End-Bearing Pile Penetrated through Clay and Rested on Sand

Name	Base Relative Density (%)	Shaft Clay OCR	Pile Length (m)
ClayOverSand 1	40	1	10, 20, 30, 40
ClayOverSand 2	50	1	10, 20, 30, 40
ClayOverSand 3	60	1	10, 20, 30, 40
ClayOverSand 4	70	1	10, 20, 30, 40
ClayOverSand 5	80	1	10, 20, 30, 40
ClayOverSand 6	90	1	10, 20, 30, 40

TABLE 3.9
Parameters of Power Functions for Piles in Clay over Sand

Name	*A*	*B*	R^2
ClayOverSand 1	17.0	−0.60	0.998
ClayOverSand 2	22.6	−0.57	0.997
ClayOverSand 3	32.3	−0.54	0.996
ClayOverSand 4	49.4	−0.50	0.997
ClayOverSand 5	82.6	−0.45	0.997
ClayOverSand 6	138	−0.40	0.997

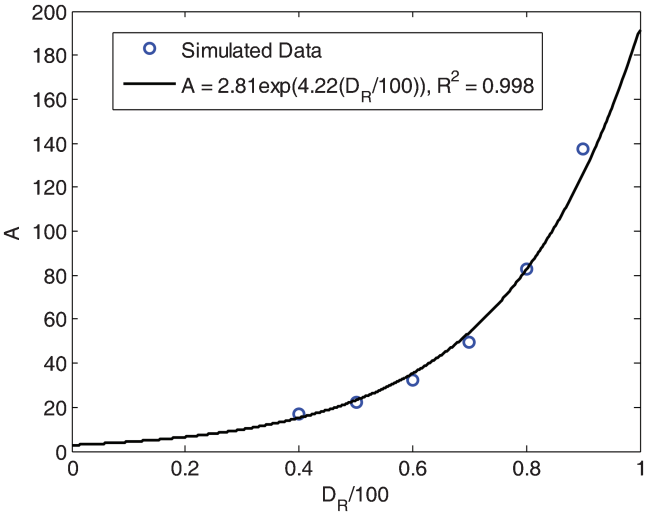

Figure 3.30 Multiplier *A* versus relative density for piles in clay over sand.

For each $\frac{W}{W_R}$ - $\frac{H}{L_R}$ pair, a specific pile driving formula can be developed based on the simulation results. A unified pile driving formula should contain these two hammer variables $\frac{W}{W_R}$ and $\frac{H}{L_R}$ adequately reproduce the

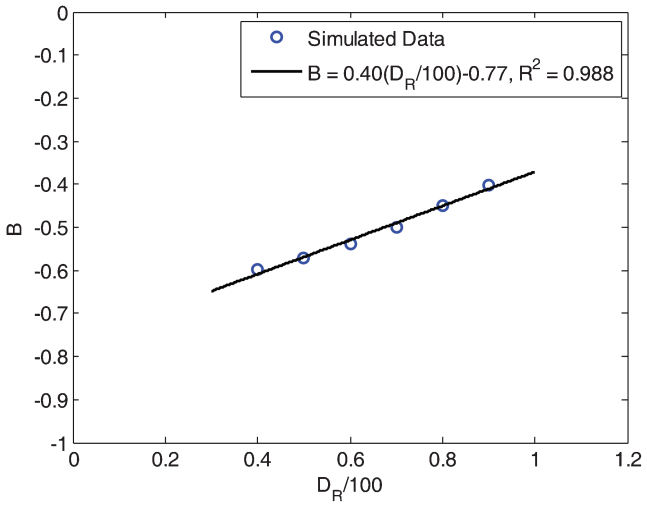

Figure 3.31 Exponent *B* versus relative density for piles in clay over sand.

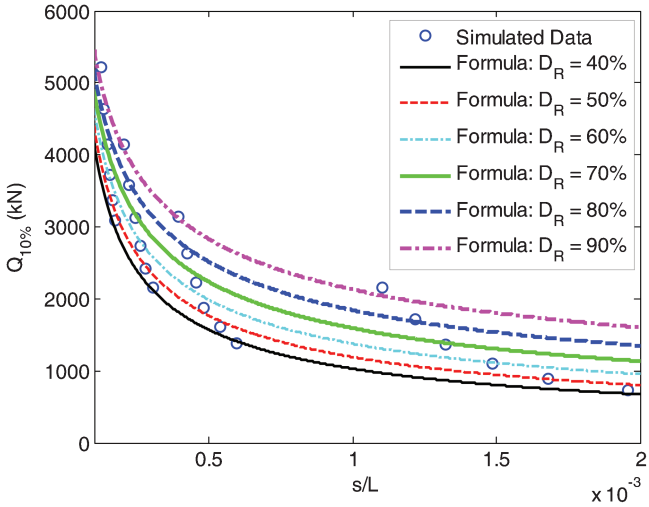

Figure 3.32 Simulated data (points) and proposed pile driving formulas (lines) of end-bearing piles through clay on sand.

individual simulations. For floating piles in sand and piles crossing a clay layer and resting on sand, the following form may be used for the pile driving formula:

$$\frac{Q_{10\%}}{p_a L_R^2} = e_h\left(a\left(\frac{W}{W_R}\right)^b\left(\frac{H}{L_R}\right)^c \exp\left(d\frac{D_R}{100}\right)\right)\left(\frac{s}{L}\right)^{e^{\frac{D_R}{100}}+f} \tag{3-18}$$

Similarly, for end-bearing piles in sand, the following form may be used for the pile driving formula:

$$\frac{Q_{10\%}}{p_a L_R^2} = e_h\left(a\left(\frac{W}{W_R}\right)^b\left(\frac{H}{L_R}\right)^c \exp\left(d\frac{D_{R_{base}}}{D_{R_{shaft}}}\right)\right)\left(\frac{s}{L}\right)^{e^{\frac{D_{R_{base}}}{D_{R_{shaft}}}}+f} \tag{3-19}$$

For floating piles in clay and end-bearing piles in clay, the following form may be used for the pile driving formula:

$$\frac{Q_L}{p_a L_R^2} = e_h\left(a\left(\frac{W}{W_R}\right)^b\left(\frac{H}{L_R}\right)^c\right)(s)^{d\frac{w}{w_0}+e} \tag{3-20}$$

Solving for variables *a*, *b*, *c*, *d*, *e*, and *f* in Equations (3-18) and (3-19) (*a*, *b*, *c*, *d*, and *e* in Equation (3-20)) is

TABLE 3.10
Hammer Parameters

	Variable						
Hammer	1	2	3	4	5	6	7
$\frac{W}{W_R}$	18.2	18.2	18.2	18.2	9.1	27.3	36.4
$\frac{H}{L_R}$	2.5	5	7.5	10	2.5	7.5	10

a typical optimization problem, for which the objective function is to obtain the maximum value for the coefficient of correlation between the data predicted from the pile driving formula and the data calculated based on the properties of the soil profile. This problem can be set, in mathematical terms, as:

$$\max(R^2) = \max\left(1 - \frac{SS_{err}}{SS_{tot}}\right) \tag{3-21}$$

where:

$SS_{tot} = \sum_i (y_i - \bar{y})^2$ = sum of squares of the difference between the pile capacity for each soil profile and the average of these capacities;

$SS_{err} = \sum_i (f_i - y_i)^2$ = sum of squares of the differences between the pile capacities predicted using the pile driving formulas and those calculated using static methods applied to the soil profile;

y_i = pile capacity calculated based on the properties of soil profile;

$\bar{y}$ = average of calculated pile capacities based on the properties of soil profiles;

f_i = pile capacity predicted by proposed pile driving formula.

This type of optimization problem can be solved by using the Microsoft Office Excel (*21*) optimization solver. A summary of the solutions to Equation (3-21) for each typical soil profile can be found in Table 3.11. The coefficient of correlation R^2 of the solution for each typical soil profile is over 0.97, which indicates the proposed pile driving formula can accurately predict the pile capacity for the soil profiles considered in this report.

For floating piles in sand, the pile driving formula is expressed in terms of five variables: the hammer efficiency, the normalized hammer weight, the normalized hammer drop height, the relative density of the sand and the pile set:

$$\frac{Q_{10\%}}{p_a L_R^2} = e_h\left(0.39\left(\frac{W}{W_R}\right)^{0.59}\left(\frac{H}{L_R}\right)^{0.38}\exp\left(2.29\frac{D_R}{100}\right)\right)\left(\frac{s}{L}\right)^{0.12\frac{D_R}{100}-0.60} \tag{3-22}$$

A comparison of the relationship between normalized pile capacity versus normalized pile set obtained from the pile driving formula and the dynamic analysis for floating piles in sand for all seven hammers is shown in Figure 3.33. The same comparison is made specifically for each hammer in Figure 3.34 through Figure 3.40. The comparisons are clearly very favorable.

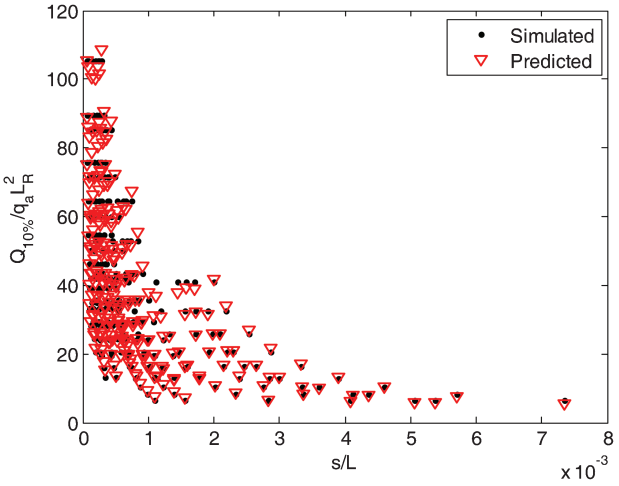

Figure 3.33 Comparison between simulated data by dynamic analysis and predicted value by proposed pile driving formula for floating piles in sand.

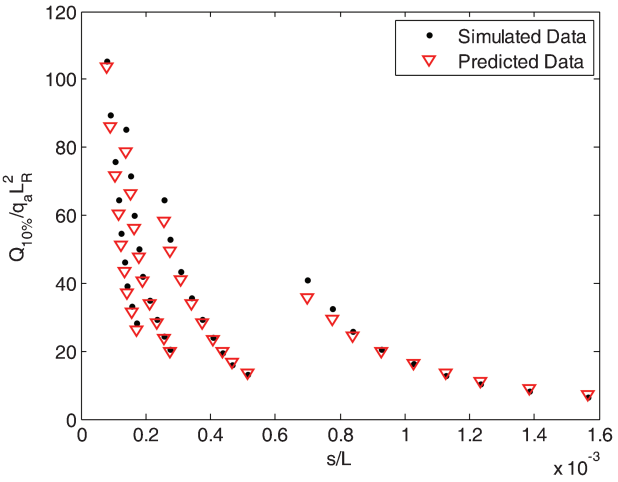

Figure 3.34 Comparison between simulated data and predicted value by proposed pile driving formula for floating piles in sand: Hammer 1 (W/W_R = 0.182 and H/L_R = 2.5).

For end-bearing piles in sand, the pile driving formula is expressed in terms of five variables: the

TABLE 3.11
Summaries of Solutions to Equation (3-21) for Typical Soil Profiles

	Variables						
Soil Profile	**a**	**b**	**c**	**d**	**e**	**f**	R^2
FLSand	0.39	0.59	0.38	2.29	0.12	−0.60	0.992
EBSand	0.46	0.53	0.33	0.55	0.033	−0.58	0.986
FLClay	0.032	0.36	1.12	−2.91	−0.73	N/A	0.991
EBClay	0.091	1.22	1.20	−2.03	−0.90	N/A	0.977
ClayOverSand	0.37	0.55	0.36	1.28	0.037	−0.58	0.980

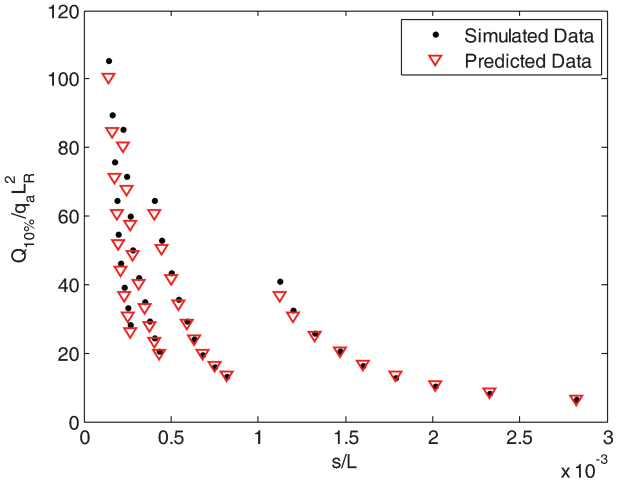

Figure 3.35 Comparison between simulated data and predicted value by proposed pile driving formula for floating piles in sand: Hammer 2 ($W/W_R = 0.182$ and $H/L_R = 5$).

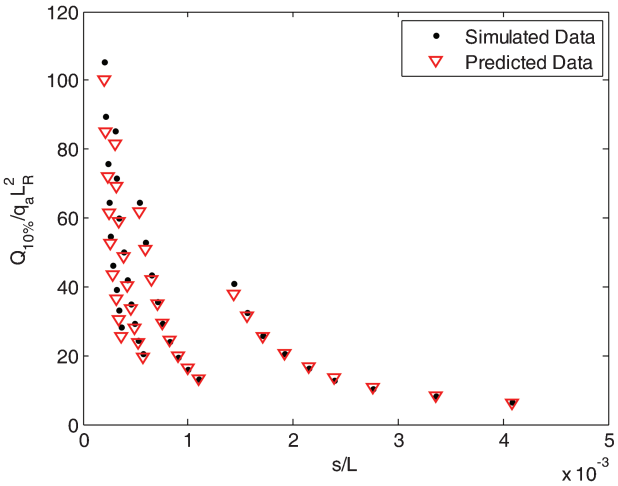

Figure 3.36 Comparison between simulated data and predicted value by proposed pile driving formula for floating piles in sand: Hammer 3 ($W/W_R = 0.182$ and $H/L_R = 7.5$).

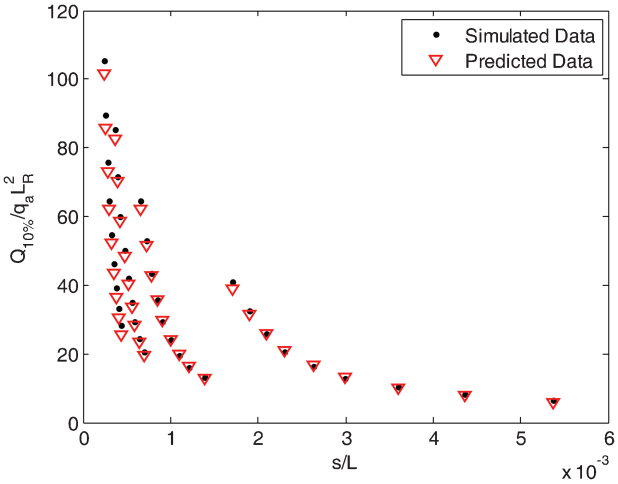

Figure 3.37 Comparison between simulated data and predicted value by proposed pile driving formula for floating piles in sand: Hammer 4 ($W/W_R = 0.182$ and $H/L_R = 10$).

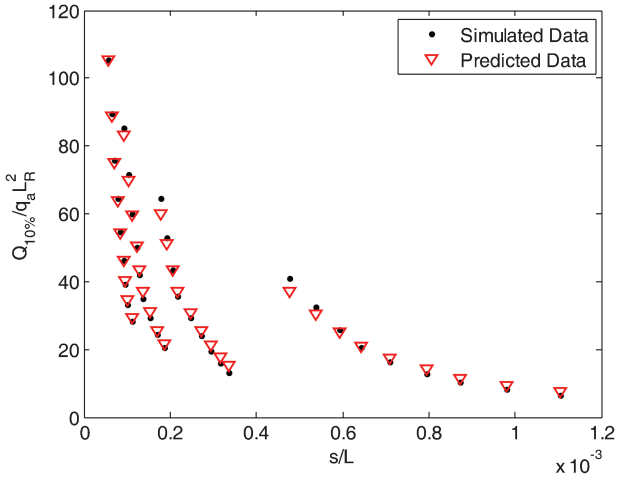

Figure 3.38 Comparison between simulated data and predicted value by proposed pile driving formula for floating piles in sand: Hammer 5 ($W/W_R = 0.091$ and $H/L_R = 5$).

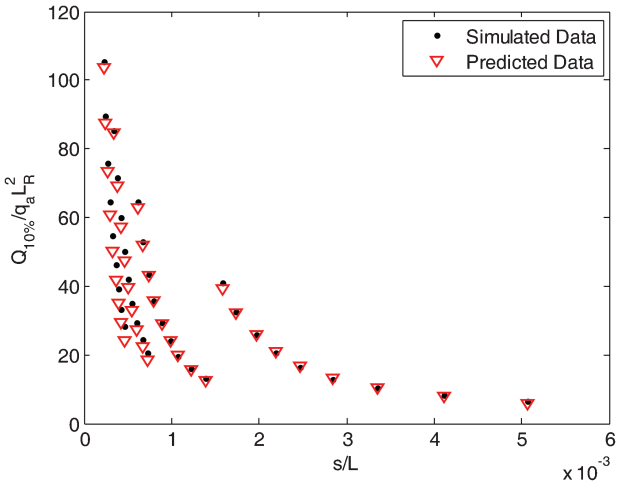

Figure 3.39 Comparison between simulated data and predicted value by proposed pile driving formula for floating piles in sand: Hammer 6 ($W/W_R = 0.273$ and $H/L_R = 5$).

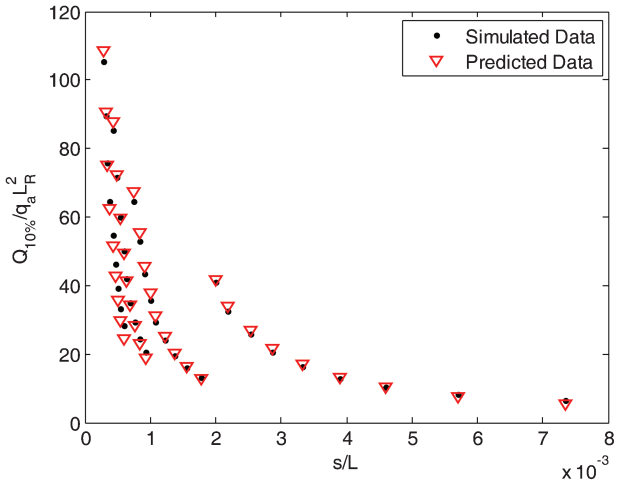

Figure 3.40 Comparison between simulated data and predicted value by proposed pile driving formula for floating piles in sand: Hammer 7 ($W/W_R = 0.364$ and $H/L_R = 5$).

hammer efficiency, the normalized hammer weight, the normalized hammer drop height, the ratio of shaft to base relative density and the pile set:

$$\frac{Q_{10\%}}{p_a L_R^2} = e_h \left(0.46 \left(\frac{W}{W_R}\right)^{0.53} \left(\frac{H}{L_R}\right)^{0.33} \exp\left(0.55 \frac{D_{R_{base}}}{D_{R_{shaft}}}\right)\right) \left(\frac{s}{L}\right)^{0.033 \frac{D_{R_{base}}}{D_{R_{shaft}}} - 0.58} \quad (3\text{-}23)$$

The normalized pile capacity versus normalized pile set relationship from the dynamic analyses and predicted using the pile driving formula are plotted together for all seven hammers in Figure 3.41. These data for hammers 1 through 7 are re-plotted separately in Figure 3.42 through Figure 3.48 to clearly show the capability and accuracy of the proposed formula for end-bearing piles in sand.

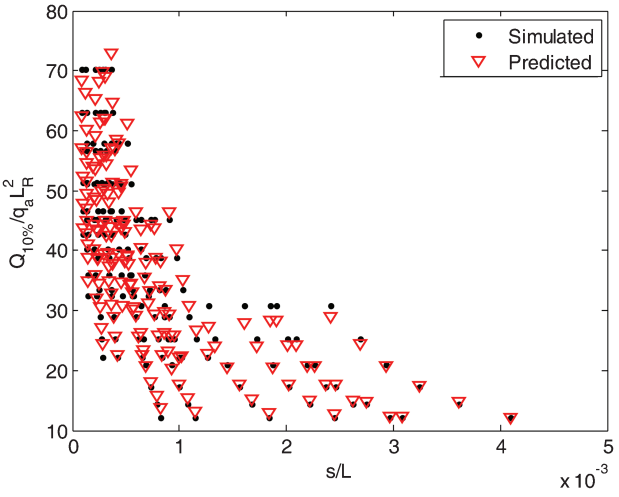

Figure 3.41 Comparison between simulated data by dynamic analysis and predicted value by proposed pile driving formula for end-bearing piles in sand.

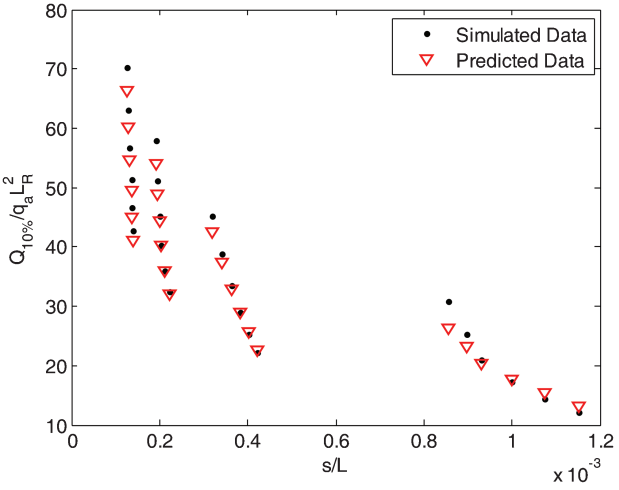

Figure 3.42 Comparison between simulated data and predicted value by proposed formula for end-bearing piles in sand: Hammer 1 ($W/W_R = 0.182$ and $H/L_R = 2.5$).

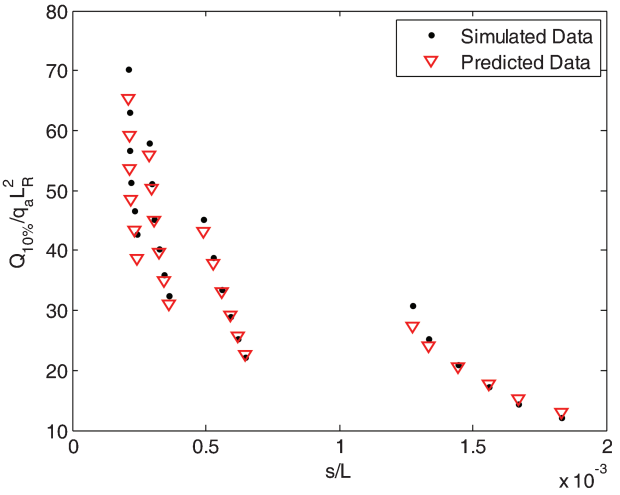

Figure 3.43 Comparison between simulated data and predicted value by proposed formula for end-bearing piles in sand: Hammer 2 ($W/W_R = 0.182$ and $H/L_R = 5$).

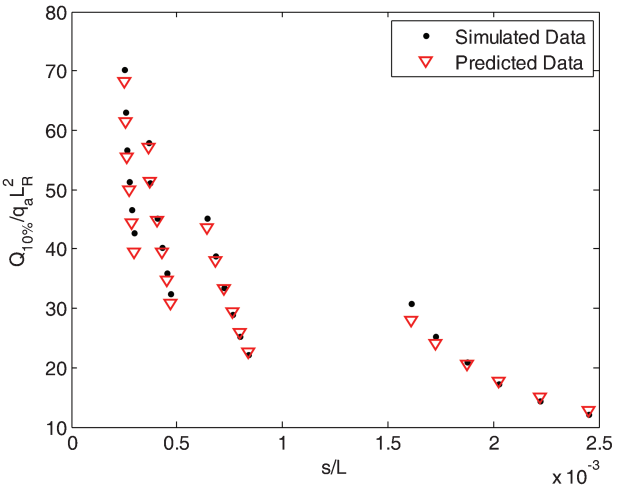

Figure 3.44 Comparison between simulated data and predicted value by proposed formula for end-bearing piles in sand: Hammer 3 ($W/W_R = 0.182$ and $H/L_R = 7.5$).

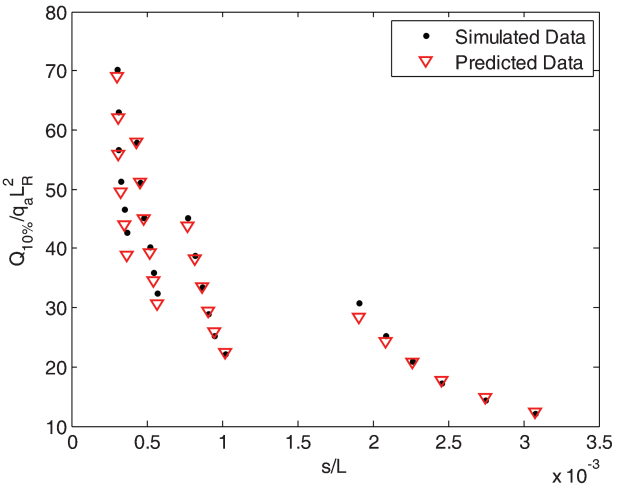

Figure 3.45 Comparison between simulated data and predicted value by proposed formula for end-bearing piles in sand: Hammer 4 ($W/W_R = 0.182$ and $H/L_R = 10$).

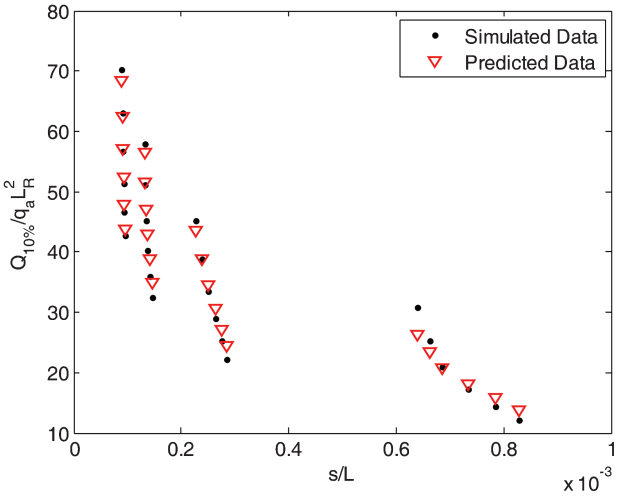

Figure 3.46 Comparison between simulated data and predicted value by proposed formula for end-bearing piles in sand: Hammer 5 ($W/W_R = 0.091$ and $H/L_R = 5$).

For floating piles in normally consolidated clay, the pile driving formula is expressed in terms of four variables: the hammer efficiency, the normalized hammer weight, the normalized hammer drop height, and the normalized pile set:

$$\frac{Q_L}{p_a L_R^2} = e_h\left(0.032\left(\frac{W}{W_R}\right)^{0.36}\left(\frac{H}{L_R}\right)^{1.12}\right)\left(\frac{s}{L_R}\right)^{-\left(2.91\frac{w}{w_R}+0.73\right)} \quad (3\text{-}24)$$

The normalized pile capacity versus normalized pile set relationship from the dynamic analyses and predicted using the pile driving formula are plotted together for all seven hammers in Figure 3.49. Specific comparisons for each hammer are shown in Figure 3.50 to Figure 3.56.

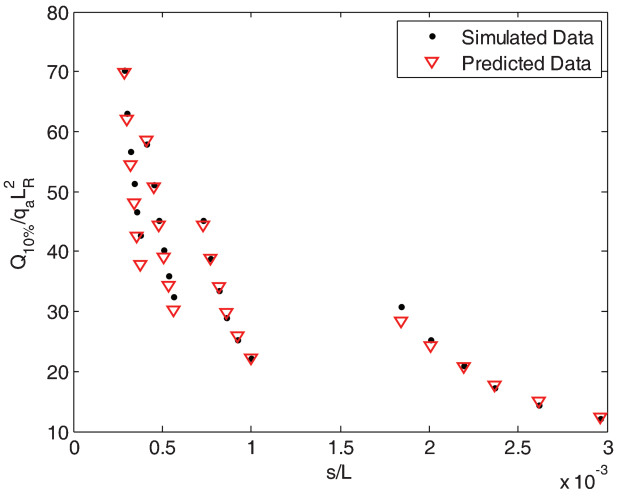

Figure 3.47 Comparison between simulated data and predicted value by proposed formula for end-bearing piles in sand: Hammer 6 ($W/W_R = 0.273$ and $H/L_R = 5$).

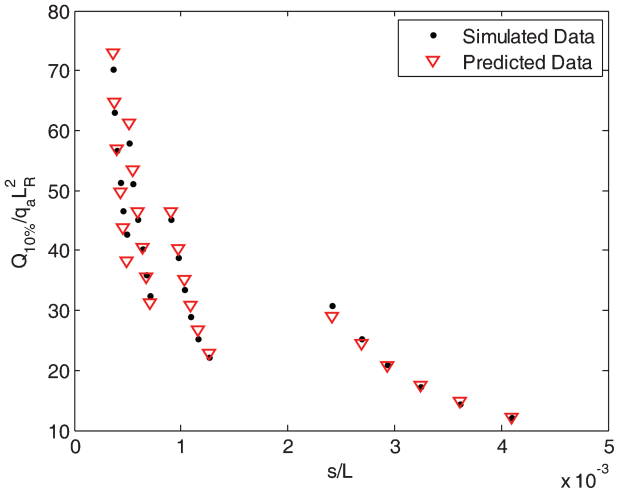

Figure 3.48 Comparison between simulated data and predicted value by proposed formula for end-bearing piles in sand: Hammer 7 ($W/W_R = 0.364$ and $H/L_R = 5$).

For piles crossing a normally consolidated clay layer and resting on an over-consolidated clay layer, the pile driving formula is expressed in terms of four variables: the hammer efficiency, the normalized hammer weight, the normalized hammer drop height, and the normalized pile set:

$$\frac{Q_L}{p_a L_R^2} = e_h\left(0.091\left(\frac{W}{W_R}\right)^{1.22}\left(\frac{H}{L_R}\right)^{1.20}\right)\left(\frac{s}{L_R}\right)^{-\left(2.03\frac{w}{w_R}+0.90\right)} \quad (3\text{-}25)$$

The normalized pile capacity versus normalized pile set relationship from the dynamic analyses and predicted using the pile driving formula are plotted together for all seven hammers in Figure 3.57. Specific

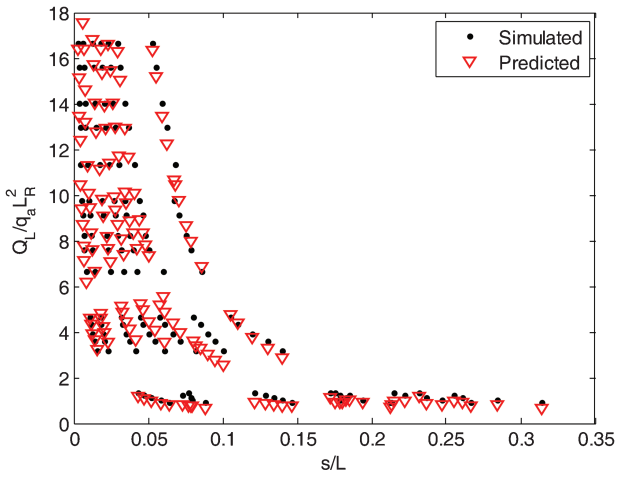

Figure 3.49 Comparison between simulated data by dynamic analysis and predicted value by proposed pile driving formula for floating piles in clay.

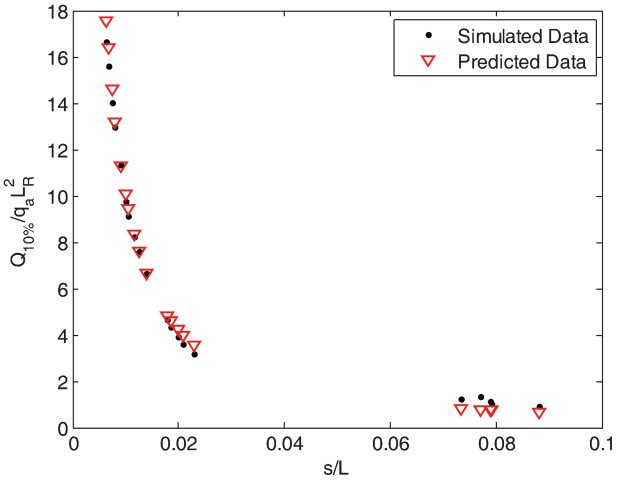

Figure 3.50 Comparison between simulated data and predicted value by proposed formula for floating piles in clay: Hammer 1 (W/W_R = 0.182 and H/L_R = 2.5).

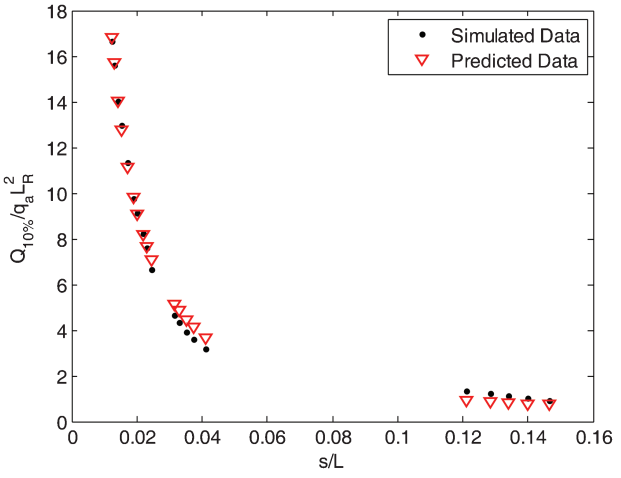

Figure 3.51 Comparison between simulated data and predicted value by proposed formula for floating piles in clay: Hammer 2 (W/W_R = 0. 182 and H/L_R = 5).

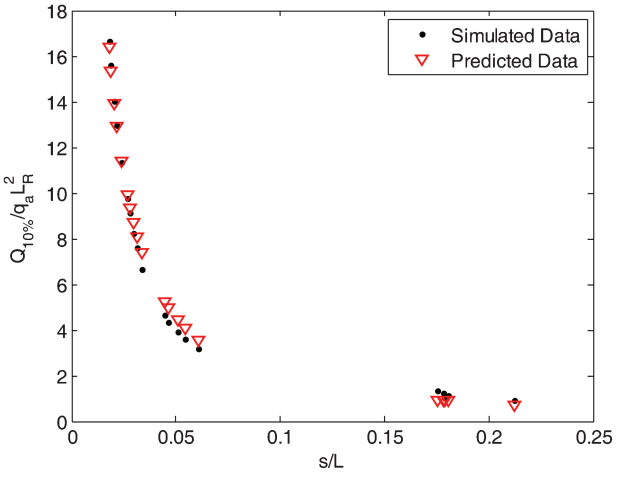

Figure 3.52 Comparison between simulated data and predicted value by proposed formula for floating piles in clay: Hammer 3 (W/W_R = 0. 182 and H/L_R = 7.5).

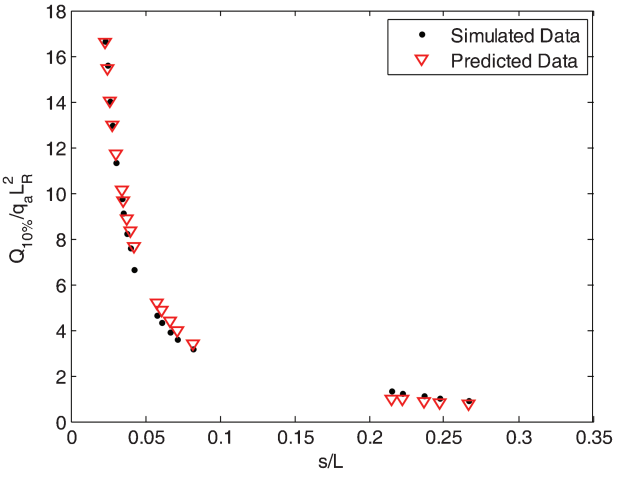

Figure 3.53 Comparison between simulated data and predicted value by proposed formula for floating piles in clay: Hammer 4 (W/W_R = 0. 182 and H/L_R = 10).

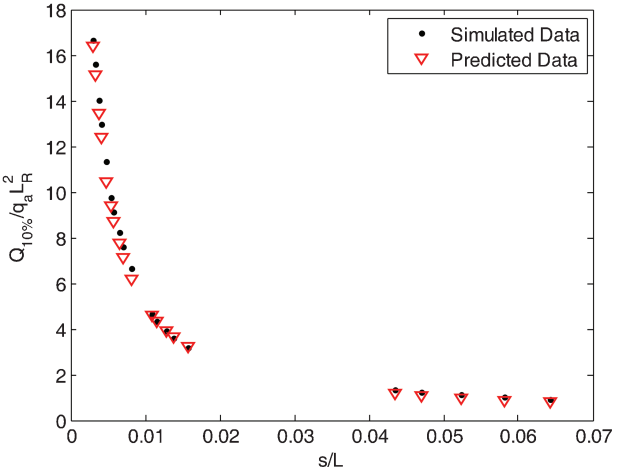

Figure 3.54 Comparison between simulated data and predicted value by proposed formula for floating piles in clay: Hammer 5 (W/W_R = 0.091 and H/L_R = 5).

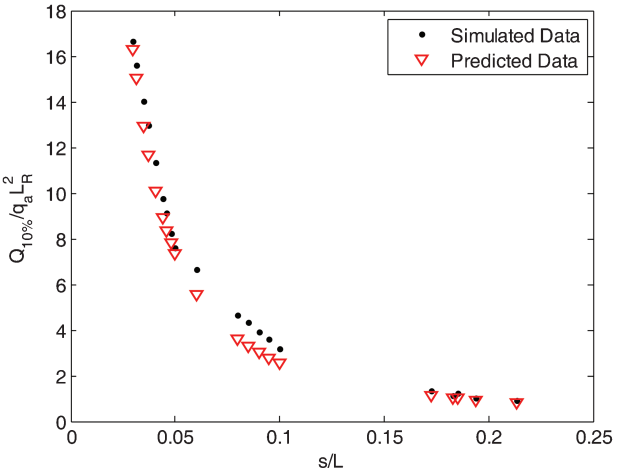

Figure 3.55 Comparison between simulated data and predicted value by proposed formula for floating piles in clay: Hammer 6 (W/W_R = 0.273 and H/L_R = 5).

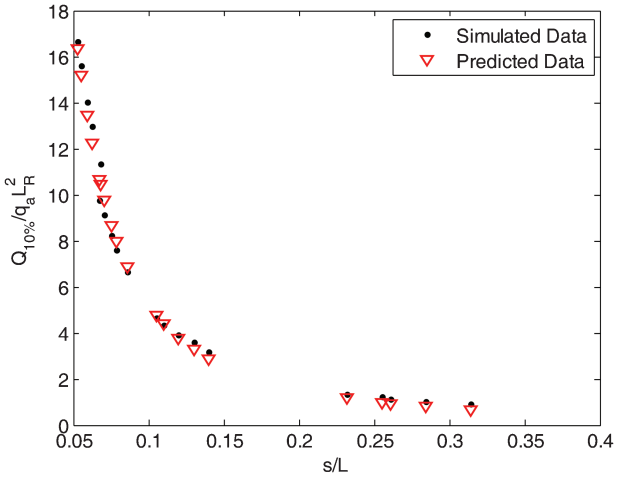

Figure 3.56 Comparison between simulated data and predicted value by proposed formula for floating piles in clay: Hammer 7 ($W/W_R = 0.364$ and $H/L_R = 5$).

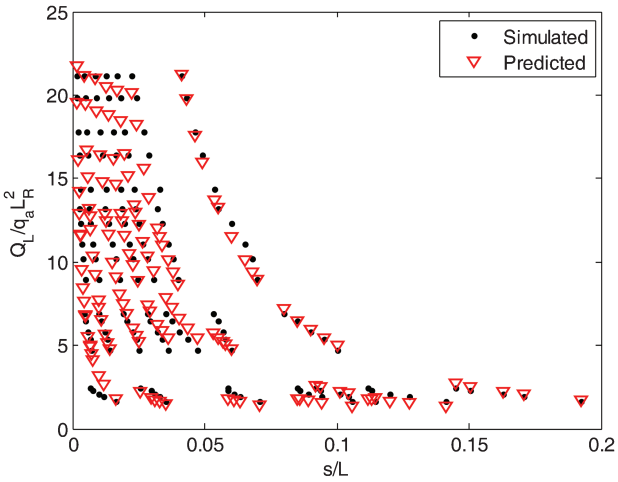

Figure 3.57 Comparison between simulated data by dynamic analysis and predicted value by proposed pile driving formula for end-bearing piles in clay.

comparisons for each hammer are shown in Figure 3.58 to Figure 3.64.

For piles crossing a clay layer and resting on a dense sand layer, the proposed pile driving formula is expressed in terms of five variables: the hammer efficiency, the normalized hammer weight, the normalized hammer drop height, the ratio of shaft relative density to base relative density and the pile set:

$$\frac{Q_{10\%}}{p_a L_R^2} = e_h\left(0.37\left(\frac{W}{W_R}\right)^{0.55}\left(\frac{H}{L_R}\right)^{0.36}\exp\left(1.28\frac{D_R}{100}\right)\right)\left(\frac{s}{L}\right)^{0.037\frac{D_R}{100}-0.58} \quad (3\text{-}26)$$

The normalized pile capacity versus normalized pile set relationship from the dynamic analyses and predicted using the pile driving formula are plotted together for all seven hammers in Figure 3.65 Specific

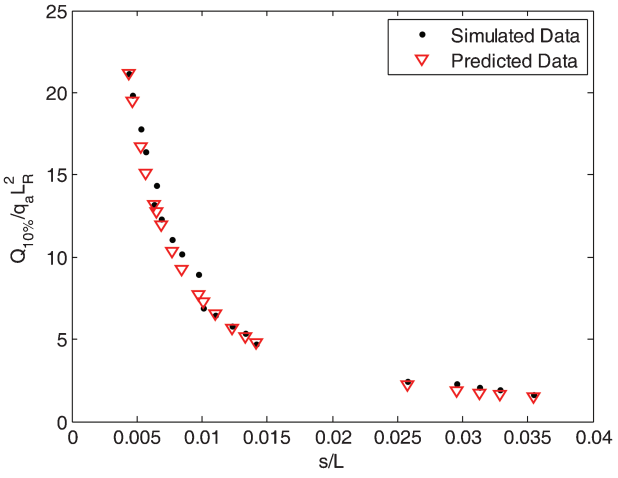

Figure 3.58 Comparison between simulated data and predicted value by proposed formula for end-bearing piles in clay: Hammer 1 ($W/W_R = 0.182$ and $H/L_R = 2.5$).

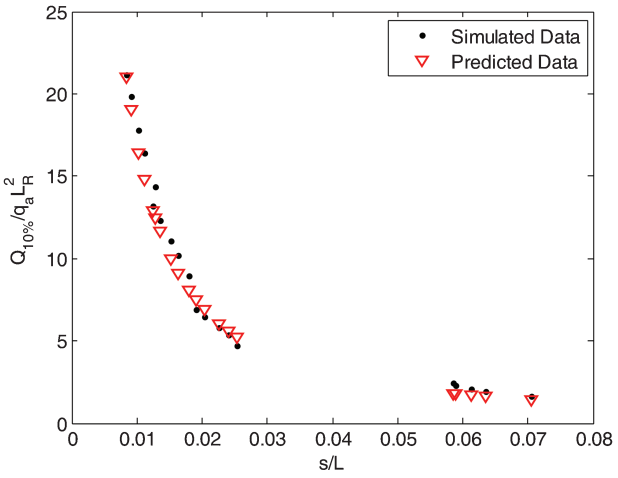

Figure 3.59 Comparison between simulated data and predicted value by proposed formula for end-bearing piles in clay: Hammer 2 ($W/W_R = 0.182$ and $H/L_R = 5$).

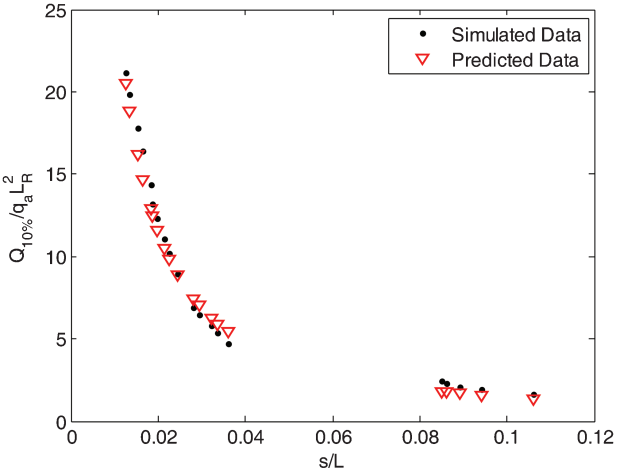

Figure 3.60 Comparison between simulated data and predicted value by proposed formula for end-bearing piles in clay: Hammer 3 ($W/W_R = 0.182$ and $H/L_R = 7.5$).

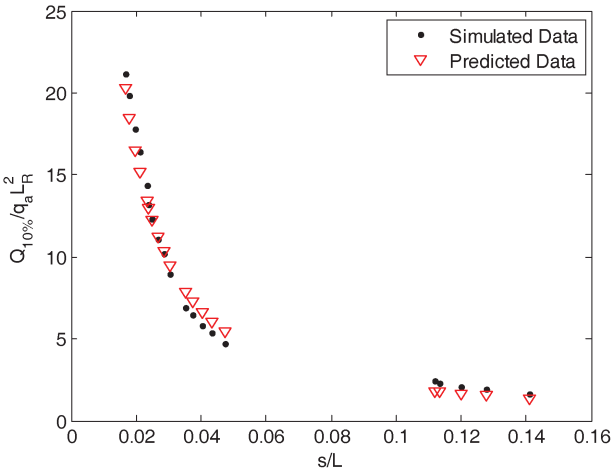

Figure 3.61 Comparison between simulated data and predicted value by proposed formula for end-bearing piles in clay: Hammer 4 (W/W_R = 0. 182 and H/L_R = 10).

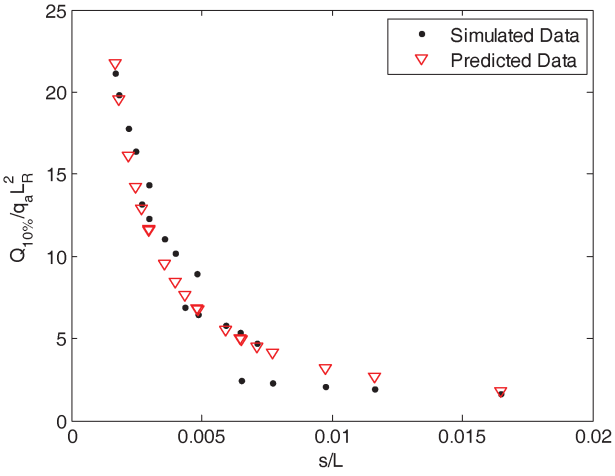

Figure 3.62 Comparison between simulated data and predicted value by proposed formula for end-bearing piles in clay: Hammer 5 (W/W_R = 0.091 and H/L_R = 5).

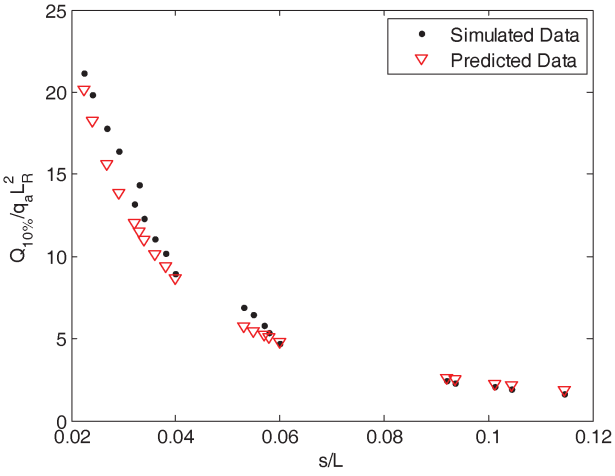

Figure 3.63 Comparison between simulated data and predicted value by proposed formula for end-bearing piles in clay: Hammer 6 (W/W_R = 0.273 and H/L_R = 5).

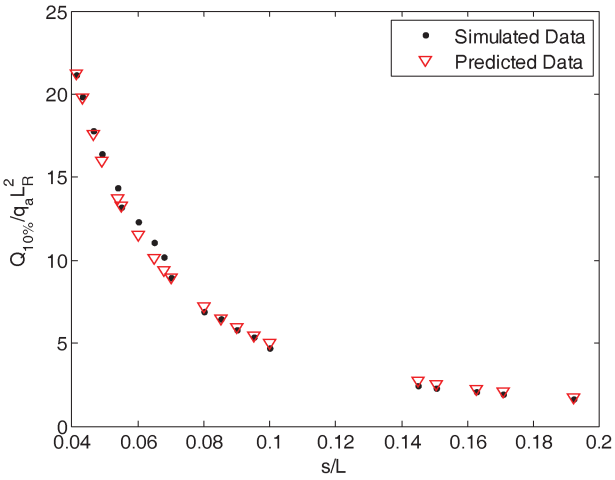

Figure 3.64 Comparison between simulated data and predicted value by proposed formula for end-bearing piles in clay: Hammer 7 (W/W_R = 0.364 and H/L_R = 5).

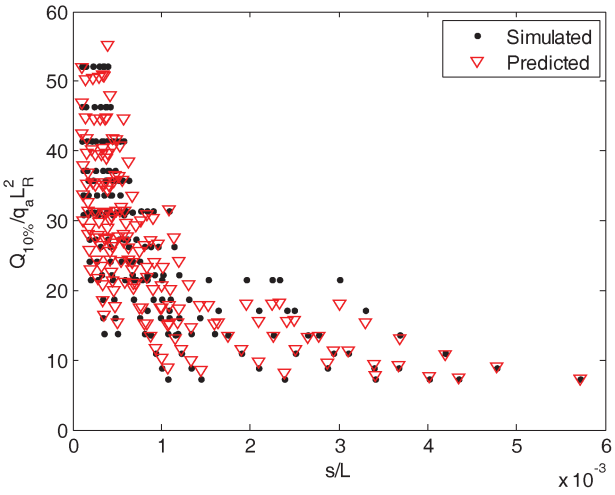

Figure 3.65 Comparison between simulated data by dynamic analysis and predicted value by proposed pile driving formula for end-bearing piles through clay on sand.

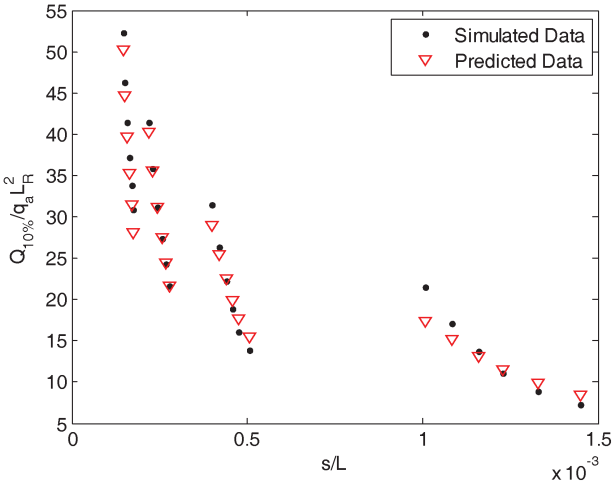

Figure 3.66 Comparison between simulated data by dynamic analysis and predicted value by proposed pile driving formula for end-bearing piles through clay on sand: Hammer 1 (W/W_R = 0.182 and H/L_R = 2.5).

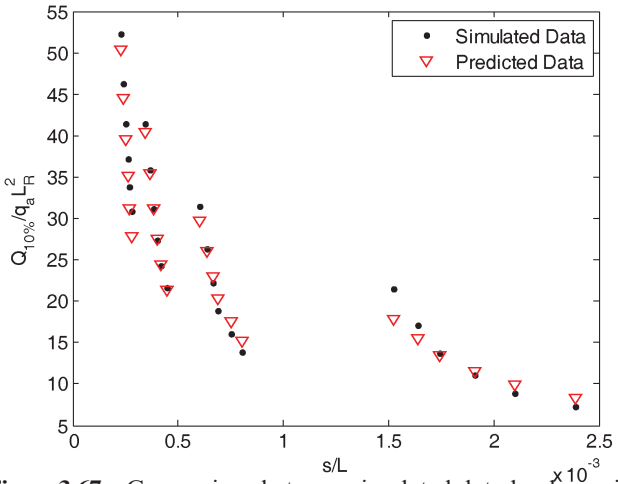

Figure 3.67 Comparison between simulated data by dynamic analysis and predicted value by proposed pile driving formula for end-bearing piles through clay on sand: Hammer 2 (W/W_R = 0. 182 and H/L_R = 5).

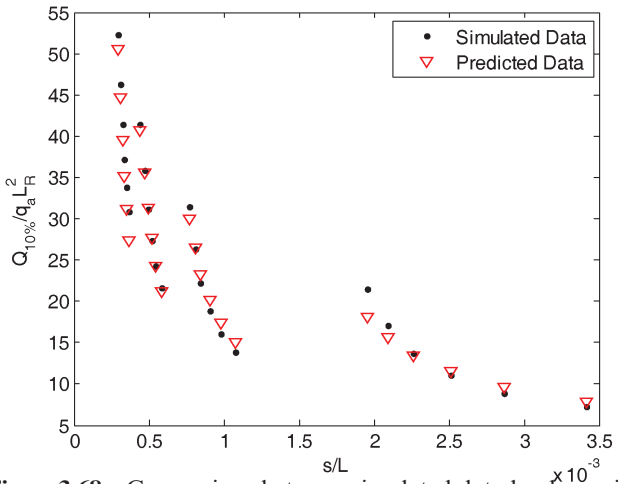

Figure 3.68 Comparison between simulated data by dynamic analysis and predicted value by proposed pile driving formula for end-bearing piles through clay on sand: Hammer 3 (W/W_R = 0. 182 and H/L_R = 7.5).

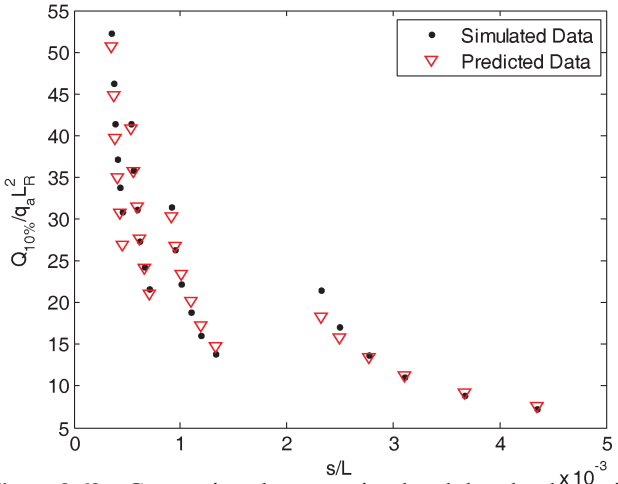

Figure 3.69 Comparison between simulated data by dynamic analysis and predicted value by proposed pile driving formula for end-bearing piles through clay on sand: Hammer 4 (W/W_R = 0. 182 and H/L_R = 10).

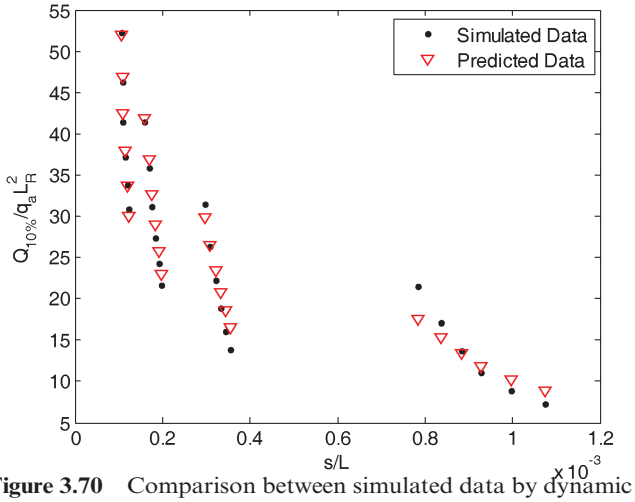

Figure 3.70 Comparison between simulated data by dynamic analysis and predicted value by proposed pile driving formula for end-bearing piles through clay on sand: Hammer 5 (W/W_R = 0.091 and H/L_R = 5).

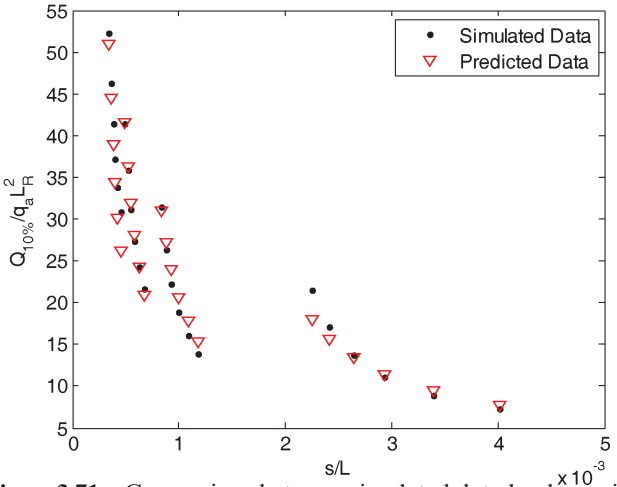

Figure 3.71 Comparison between simulated data by dynamic analysis and predicted value by proposed pile driving formula for end-bearing piles through clay on sand: Hammer 6 (W/W_R = 0.273 and H/L_R = 5).

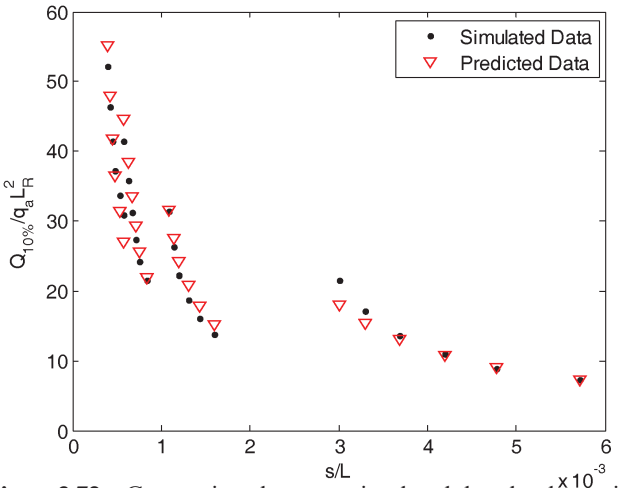

Figure 3.72 Comparison between simulated data by dynamic analysis and predicted value by proposed pile driving formula for end-bearing piles through clay on sand: Hammer 7 (W/W_R = 0.364 and H/L_R = 5).

comparisons for each hammer are shown in Figure 3.66 to Figure 3.72.

4. CASE STUDY

In the final report of SPR-2856 (*8*), driven piles in Lagrange County and Jasper County are used to validate the Purdue pile driving analysis by comparing the measured and predicted pile set. In this chapter, we will continue using these two site histories to test the proposed pile driving formulas proposed in Chapter 3.

4.1 Lagrange County

Full-scale pile load tests were performed over Pigeon River in Lagrange County, Indiana. Details of this project can be found in Paik et al. (*22*). We will focus on the closed-ended steel pipe pile with a length 8.24m and outer and inner diameters of 356mm and 331mm respectively. The hammer used was an ICE-42S single acting hammer with a rated maximum driving energy of 56.7kNm.

The soil profile consisted of loose gravelly sand (D_R = 30%) down to 3m, followed by dense gravelly sand with D_R = 80%. The pile capacity at the end of the load test for the close-ended pile is 1.77×10^3kN. According to the driving log, the observed final pile set was 10mm (*8*). The closed-ended pile was driven to a depth of 6.87m.

To use the end-bearing pile formula in sand, the relative density assumed for the base layer is 80% while the average relative density assumed for the shaft is 58%, which is obtained as follows:

$$(3 \times 30\% + 3.87 \times 80\%)/6.87 = 58\% \qquad (4\text{-}1)$$

The pile length is 6.87m, with pile set 10mm. The calculated pile capacity of the close-ended pile under this scenario is 1.49×10^3kN. The CAPWAP predictions based on a re-strike test performed 126 days after the end of pile driving is 903kN, which underestimates the static load capacity of this pile, which was as 1.77×10^3 kN.

The Gates formula (*1*) is a purely empirical relationship between the pile set and pile capacity, not considering any information about the pile and the soil. It is given follows:

$$Q_u = a\sqrt{e_h E_h}(b - \log(s)) \qquad (4\text{-}2)$$

where

Q_u - Pile capacity, kN or kips;

s - Pile set, mm;

e_h - Efficiency of the hammer, 0.75 for drop and 0.85 for all other hammers;

TABLE 4.1
Parameters for *a* and *b* in Gates Formula for SI and USCU

	s	*a*	*b*
SI Unit	inch	27	1.0
English Unit	mm	105	2.4

TABLE 4.2
Measured and Predicted Pile Capacity in Lagrange County

Method of Determination	Pile Capacity (kN)
Static Load Test	1.77×10^3
End-Bearing Pile in Sand Formula	1.49×10^3
Gates Formula	8.89×10^2
CAPWAP	9.03×10^2

E_h - Maximum driving energy of the hammer, kN-m or kips-ft;

a and b –Values shown in Table 4.1.

The value directly calculated by the Gates formula (equation (4-2)) is the capacity of the pile. A factor of safety of 3 was suggested by Bowles (*2*) to obtain the allowable pile capacity in piling engineering design. The calculated pile capacity directly from Gates formula without considering the factor of safety is 889kN with pile set of 10mm, which is conservative when compared to the pile capacity of 1.77×10^3kN from the static load test. The measured and predicted pile capacities in Lagrange County are compared in Table 4.2.

4.2 Jasper County

Another full-scale steel pipe pile was installed in Jasper County, Indiana. Details of this project can be found in Loukidis et al. (*8*) and Seo et al. (*23*). The closed-ended steel pipe pile was 17.5m long with an outer diameter 356mm and 12.7mm wall thickness. An ICE-42S single acting hammer with rated maximum driving energy 56.8 kNm was used to drive the pile.

The split spoon samples obtained from different depths showed that the soil profile consisted mainly of a thick deposit of clayey silt and silty clay down to 25m depth. The test pile rested on a very dense silt layer. According to Pile Driving Analyzer (PDA) data, the measured pile set was 9mm when the closed-ended pile was driven to a depth of 17.5m (*8*). By using the formula for piles penetrating through clay and bearing on sand, we get the pile capacity for this pile as 2.17×10^3kN with an estimation of relative density of the base layer as 50%. The pile capacity at the end of the load test on the close-ended pile was 2.14×10^3kN (*23*).

The pile capacity calculated from the Gates formula is 918kN, which is too conservative compared with the static pile capacity as 2.14×10^3kN. The CAPWAP predictions based on a re-strike test performed 126 days after the end of pile driving is 1.49×10^3kN (*23*). The measured and predicted pile capacities are listed in Table 4.3.

TABLE 4.3
Measured and Predicted Pile Capacity in Jasper County

Method of Determination	**Pile Capacity (kN)**
Static Load Test	2.14×10^3
Clay over Sand Formula	2.17×10^3
Gates Formula	9.18×10^2
CAPWAP Prediction	1.49×10^3

TABLE 5.1
Summary of Pile Driving Formulas for Floating and End-Bearing Piles in Typical Soil Deposits

Soil Type	Pile Type	Formula
Sand	Floating	$\frac{Q_{10\%}}{p_a L_R^2} = e_h\left(0.39\left(\frac{W}{W_R}\right)^{0.59}\left(\frac{H}{L_R}\right)^{0.38}\exp\left(2.29\frac{D_R}{100}\right)\right)\left(\frac{s}{L}\right)^{0.12\frac{D_R}{100}-0.60}$
	End-bearing	$\frac{Q_{10\%}}{p_a L_R^2} = e_h\left(0.46\left(\frac{W}{W_R}\right)^{0.53}\left(\frac{H}{L_R}\right)^{0.33}\exp\left(0.55\frac{D_{R_{base}}}{D_{R_{shaft}}}\right)\right)\left(\frac{s}{L}\right)^{0.033\frac{D_{R_{base}}}{D_{R_{shaft}}}-0.58}$
Clay	Floating	$\frac{Q_L}{p_a L_R^2} = e_h\left(0.032\left(\frac{W}{W_R}\right)^{0.36}\left(\frac{H}{L_R}\right)^{1.12}\right)\left(\frac{s}{L_R}\right)^{-\left(2.91\frac{w}{w_R}+0.73\right)}$
	End-bearing	$\frac{Q_L}{p_a L_R^2} = e_h\left(0.091\left(\frac{W}{W_R}\right)^{1.22}\left(\frac{H}{L_R}\right)^{1.20}\right)\left(\frac{s}{L_R}\right)^{-\left(2.03\frac{w}{w_R}+0.90\right)}$
Shaft: Clay Base: Sand		$\frac{Q_{10\%}}{p_a L_R^2} = e_h\left(0.37\left(\frac{W}{W_R}\right)^{0.55}\left(\frac{H}{L_R}\right)^{0.36}\exp\left(1.28\frac{D_R}{100}\right)\right)\left(\frac{s}{L}\right)^{0.037\frac{D_R}{100}-0.58}$

5. SUMMARY AND CONCLUSION

The main goal of this study was to propose a series of pile driving formulas considering different typical soil profiles. These formulas, which are based on analysis that has been proven to be reasonably accurate, offer an alternative to pile dynamic tests in low- to average-budget projects. Chapter 2 discussed the determination or estimation of each parameter appearing in the advanced pile dynamics analysis model. Chapter 3 described the development of the proposed pile driving formulas in sandy and clayey soils both for floating and end-bearing piles. The case studies of Chapter 4 show that traditional pile driving formulas are very conservative and that the proposed formulas performed well. The pile driving formulas developed in this study are summarized in Table 5.1. Until they can be further verified, they should be used with caution.

In Table 5.1, the reference values are defined as:

Reference force: $W_R = 100\text{kN} = 2.25\times10^3\text{lbf} = 22.5\text{kips}$;

Reference length: $L_R = 1\text{m} = 3.28\text{ft} = 39.3\text{in}$;

Reference stress: $p_a = 100\text{kPa} = 0.1\text{MPa} = 1\text{kgf/cm}^2 = 1\text{tsf}$.

REFERENCES

1. Gates, M. Empirical Formula for Predicting Pile Bearing Capacity. *Civil Engineering*, ASCE, Vol. 27, No. 3, March, 1957, pp. 65–66.
2. Bowles, E. J. *Foundation Analysis and Design*. McGraw Hill, New York, 1996.
3. Olson, R. E., and K. S. Flaate. Pile Driving Formulas for Friction Piles in Sand. *JSMFD*, ASCE, Vol. 93, No. SM6, Nov. 1967, pp. 279–296.
4. Chellis, R. D. *Pile Foundations*, 2nd ed. McGraw-Hill, New York, 1961.
5. ENR. Michigan Pile Test Program Test Results Are Released. *Eng. News-Record*, May 20, 1965, pp. 26–28, 33–34.
6. AASHTO. *Standard Specifications for Highway Bridges*. 14th ed. American Association of State Highway and Transportation Officials, Washington, D.C., 1990.
7. Smith, E. A. L. Pile-Driving Analysis by the Wave Equation. *Journal Soil Mechanics and Foundations Division ASCE*, Vol. 86, No. EM4, 1960, pp. 35–61.
8. Loukidis, D., R. Salgado, and G. Abou-Jaoude. *Assessment of Axially-Loaded Pile Dynamic Design Methods and Review of INDOT Axially-Loaded Pile Design Procedure*. Publication FHWA/IN/JTRP-2008/06. Indiana Department of Transportation and Purdue University, West Lafayette, Indiana, 2008. doi: 10.5703/1288284313450.
9. Randolph, M. F., and H. A. Simons. An Improved Soil Model for One-Dimensional Pile Driving Analysis. *Proceedings of the 3rd International Conference of Numerical Methods in Offshore Piling*, Nantes France, 3–17, 1986.
10. Hardin, B. O., and W. L. Black. Vibration Modulus of Normally Consolidated Clay. *Journal Soil Mechanics and Foundation Division ASCE*, Vol. 94, No. SM2, 1968, pp. 353–369.
11. Hardin B. O., and V. P. Drnevich. Shear Modulus and Damping in Soils: Design Equations and Curves. *Journal of the Soil Mechanics and Foundations Division*, Vol. 98, No. 7, pp. 667–692.
12. Coyle, H. M., G. C. and Gibson. Empirical Damping Constants for Sands and Clays. *Journal Soil Mechanics and Foundations Division ASCE*, Vol. 96, No. SM3, 1970, pp. 949–965.
13. Randolph, M. F. Science and Empiricism in Pile Foundation Design. 43rd Rankine Lecture. *Geotechnique*, Vol. 54, No. 1, 2003.
14. Lee, S. L., Y. K. Chow, G. P. Karunaratne, and K. Y. Wong. Rational Wave Equation For Pile-Driving Analysis. *Journal of Geotechnical Engineering*, Vol. 114,

No. 3, 1988, pp. 306–325. doi: 10.1061/(ASCE)0733-9410(1988)114:3(306).
15. Lehane, B. M., J. A. Schneider, and X. Xu. The UWA-05 Method for Prediction of Axial Capacity of Driven Piles in Sand. *Proceedings of International Symposium on Frontiers in Offshore Geotechnics*, Perth, Australia, 2005, pp. 683–689.
16. Jardine, R. J., F. C. Chow, R. F. Overy, and J. R. Standing. *ICP Design Methods for Driven Piles in Sand and Clays*. Thomas Telford, London, 2005. doi: 10.1680/idmfdpisac.32729.
17. Basu, P., R. Salgado, M. Prezzi, and T. Chakraborty. *A Method For Accounting For Pile Setup and Relaxation in Pile Design and Quality Assurance*. Publication FHWA/IN/JTRP-2009/24. Joint Transportation Research Program, Indiana Department of Transportation and Purdue University, West Lafayette, Indiana, 2009. doi: 10.5703/1288284314282.
18. Salgado, R., and M. Prezzi. Computation of Cavity Expansion Pressure and Penetration Resistance in Sands. *International Journal of Geomechanics*, Vol. 7, No. 4, 2007, pp. 251–265. doi: 10.1061/(ASCE)1532-3641(2007)7:4(251).
19. Salgado, R. *The Engineering of Foundations*. McGraw Hill, New York, 2008.
20. ICEUSA. *ICE Model 42S Fuel-Injected Diesel Pile Hammers*. 2011. http://www.iceusa.com/files/uploads/75EE1F17-9106-4590-8021-AD86B608D08E.pdf. Retrieved 15 August, 2011.
21. Microsoft Corporation. *Introduction to Optimization with the Excel Solver Tool*. 2007. http://office.microsoft.com/en-us/excel-help/introduction-to-optimization-with-the-excel-solver-tool-HA001124595.aspx. Retrieved 19 February, 2012.
22. Paik, K., R. Salgado, J. Lee, and B. Kim. Behavior of Open and Closed-ended Piles Driven into Sands. *Journal of Geotechnical and Geoenvironmental Engineering*, Vol. 129, No. 4, 2003, pp. 296–306.
23. Seo, H., I. Z. Yildirim, and M. Prezzi. Assessment of the Axial Load Response of an H Pile Driven in Multilayered Soil. *Journal of Geotechnical and Geoenvironmental Engineering*, Vol. 135, No. 12, 2009, pp. 1789–1804. doi: 10.1061/(ASCE)GT.1943-5606.0000156.